Calhoun: The NPS Institutional Archive

DSpace Repository

Theses and Dissertations | 1. Thesis and Dissertation Collection, all items

1996-09

Use of the symmetrical number system in resolving undersampling aliases

Leino, Richard E.

Monterey, California. Naval Postgraduate School

http://hdl.handle.net/10945/32261

This publication is a work of the U.S. Government as defined in Title 17, United States Code, Section 101. Copyright protection is not available for this work in the United States.

Downloaded from NPS Archive: Calhoun

http://www.nps.edu/library

Calhoun is the Naval Postgraduate School's public access digital repository for research materials and institutional publications created by the NPS community. Calhoun is named for Professor of Mathematics Guy K. Calhoun, NPS's first appointed -- and published -- scholarly author.

Dudley Knox Library / Naval Postgraduate School
411 Dyer Road / 1 University Circle
Monterey, California USA 93943

NAVAL POSTGRADUATE SCHOOL
Monterey, California

THESIS

USE OF THE SYMMETRICAL NUMBER SYSTEM IN RESOLVING UNDERSAMPLING ALIASES

by

Richard E. Leino

September 1996

Thesis Advisor: Phillip E. Pace

Approved for public release; distribution unlimited.

19970109 011

DTIC QUALITY INSPECTED 1

REPORT DOCUMENTATION PAGE

Form Approved
OMB No. 0704-0188

Public reporting burden for the collection of information is estimated to average 1 hour per response, including the time for reviewing instructions, searching existing data sources, gathering and maintaining the data needed, and completing and reviewing the collection of information. Send comments regarding this burden estimate or any other aspect of this collection of information, including suggestions for reducing this burden to Washington Headquarters Services, Directorate for Information Operations and Reports, 1215 Jefferson Davis Highway, Suite 1204, Arlington VA 22202-4302, and to the Office of Management and Budget, Paperwork Reduction Project (0704-0188), Washington DC 20503.

1. AGENCY USE ONLY (Leave blank)	2. REPORT DATE	3. REPORT TYPE AND DATES COVERED
	September 1996	Master's Thesis

4. TITLE AND SUBTITLE
USE OF THE SYMMETRICAL NUMBER SYSTEM IN RESOLVING UNDERSAMPLING ALIASES

5. FUNDING NUMBERS

6. AUTHOR(S)
Leino, Richard E.

7. PERFORMING ORGANIZATION NAME(S) AND ADDRESS(ES)
Naval Postgraduate School
Monterey, CA 93943-5000

8. PERFORMING ORGANIZATION REPORT NUMBER

9. SPONSORING/MONITORING AGENCY NAME(S) AND ADDRESS(ES)

10. SPONSORING/MONITORING AGENCY REPORT NUMBER

11. SUPPLEMENTARY NOTES
The views expressed in this report are those of the author and do not reflect the official policy or position of the Department of Defense or the United States Government.

12a. DISTRIBUTION/AVAILABILITY STATEMENT
Approved for public release; distribution unlimited.

12b. DISTRIBUTION CODE

13. ABSTRACT (Maximum 200 words)

Two algorithms are presented which allow for the unambiguous resolution of multiple undersampled frequency components in a signal. Digital signal processing is usually governed by the Nyquist criterion which limits the amount of information that can be unambiguously stored and recovered digitally to a spectral width no larger than half the sampling frequency. Both algorithms resolve a spectrum beyond Nyquist by using additional information. The first method samples a signal more than once using a different sampling frequency each time. The second method utilizes a single sampling frequency which is used to sample both the signal and a band-limited version of the signal. When using multiple sampling frequencies, each sampling frequency yields a digital sequence which, in turn, has a unique spectrum when the Discrete Fourier Transform (DFT) is applied. The bin and amplitude information from each of the resulting undersampled spectra is then recombined to resolve the original spectrum. In like manner, when using a single sampling frequency the spectra of both the signal and its band-limited version are recombined to obtain the solution. Given a sampling frequency, both algorithms allow for the unambiguous resolution of a signal with a spectral width at least twice as large as that predicted by Nyquist.

14. SUBJECT TERMS

15. NUMBER OF PAGES
83

16. PRICE CODE

17. SECURITY CLASSIFICATION OF REPORT	18. SECURITY CLASSIFICATION OF THIS PAGE	19. SECURITY CLASSIFICATION OF ABSTRACT	20. LIMITATION OF ABSTRACT
Unclassified	Unclassified	Unclassified	UL

Approved for public release; distribution is unlimited

USE OF THE SYMMETRICAL NUMBER SYSTEM IN RESOLVING UNDERSAMPLING ALIASES

Richard E. Leino
Captain, United States Marine Corps
B.S., Rensselaer Polytechnic Institute, 1990

Submitted in partial fulfillment of the
requirements for the degreee of

MASTER OF SCIENCE IN ELECTRICAL ENGINEERING

from the

NAVAL POSTGRADUATE SCHOOL
September 1996

Author: [redacted]
Richard E. Leino

Approved by: [redacted]
Phillip E. Pace, Advisor

[redacted]
David Styer, Second Reader

[redacted]
Herschel H. Loomis, Jr., Chairman
Department of Electrical and Computer Engineering

ABSTRACT

Two algorithms are presented which allow for the unambiguous resolution of multiple undersampled frequency components in a signal. Digital signal processing is usually governed by the Nyquist criterion which limits the amount of information that can be unambiguously stored and recovered digitally to a spectral width no larger than half the sampling frequency. Both algorithms resolve a spectrum beyond Nyquist by using additional information. The first method samples a signal more than once using a different sampling frequency each time. The second method utilizes a single sampling frequency which is used to sample both the signal and a band-limited version of the signal. When using multiple sampling frequencies, each sampling frequency yields a digital sequence which, in turn, has a unique spectrum when the Discrete Fourier Transform (DFT) is applied. The bin and amplitude information from each of the resulting undersampled spectra is then recombined to resolve the original spectrum. In like manner, when using a single sampling frequency the spectra of both the signal and its band-limited version are recombined to obtain the solution. Given a sampling frequency, both algorithms allow for the unambiguous resolution of a signal with a spectral width at least twice as large as that predicted by Nyquist.

TABLE OF CONTENTS

I. INTRODUCTION 1

A. BACKGROUND 1

B. UNDERSAMPLING 1

C. PRINCIPLE CONTRIBUTION 2

D. THESIS OUTLINE 3

II. THE SYMMETRICAL NUMBER SYSTEM 5

A. DEFINING THE SNS WAVEFORM 5

B. DYNAMIC RANGE OF AN SNS SYSTEM 6

1. Example of the SNS Dynamic Range 6

C. PROOF OF THE SNS DYNAMIC RANGE 7

1. Proof of Theorem 2.1a. 8

a. Case I 8

b. Case II 9

2. Proof of Theorem 2.1b. 11

a. Case I 12

b. Case II 12

III. DFT AND SNS RELATIONSHIP 15

A. DIGITAL SAMPLING AND ALIASING 15

B. DIGITAL FREQUENCY MAPPING 15

C. DFT BINS AND THE SNS 16

D. ILLUSTRATING THE RELATIONSHIP 17

IV. RESOLVING THE TWO CHANNEL CASE 21

A. THE GENERAL SETUP 21

B. SET-UP FOR A PARTICULAR TWO CHANNEL RECEIVER . 23

C. SOLVING A PARTICULAR CASE - THE WORK OF THE ALGORITHM 23
D. SPECIAL CASES 23
V. RESOLVING THE THREE CHANNEL CASE 25
A. GENERAL SETUP 25
B. SOLVING A THREE CHANNEL EXAMPLE 25
VI. RESOLUTION OF TWO UNDERSAMPLED FREQUENCIES 27
A. DFT AMPLITUDE NORMALIZATION 27
B. BENEFITS OF NORMALIZATION 27
C. SPECIAL CASE 28
VII. INTRODUCTION TO RESOLVING MULTIPLE FREQUENCIES . . 31
A. SETTING UP THE SOLUTION 31
B. EXAMPLE 33
VIII. RESOLVING MULTIPLE FREQUENCIES: FIRST ALGORITHM . . 37
A. CONSIDERING RANDOM PHASE SIGNALS 37
1. Illustration of Random Phase by Example 37
2. The Imaginary Component 38
B. SOLVING FOR REAL AND IMAGINARY COMPONENTS . . . 38
C. THE PIVOTAL FREQUENCY 40
D. EXAMPLE 40
E. REDUCING THE COMPUTING COST 43
F. GENERALIZING THE SOLUTION 44
IX. RESOLVING MULTIPLE FREQUENCIES: SECOND ALGORITHM 47
A. BACKGROUND 47
B. USING THE BANDLIMITED SPECTRUM 47
1. Recovering the First Half of the Spectrum 48

2. Recovering the Other Half of the Spectrum 48
C. GENERAL SOLUTION 49
X. PROBLEMS WITH THE SOLUTION 53
A. SIGNALS THAT CAUSE DFT LEAKAGE 53
B. DFT LEAKAGE EXAMPLES 53
1. Algorithm of Theorem 8.1 53
2. Algorithm of Theorem 9.1 53
C. LEAKAGE AND SOLUTION INSTABILITY 54
D. SOLVING THE PROBLEM? 54
XI. CONCLUDING REMARKS 63
LIST OF REFERENCES 65
INITIAL DISTRIBUTION LIST 67

LIST OF FIGURES

3.1 a)Z-plane mapping of an input analog signal. b) sampled frequency output. 16

3.2 a)DFT mapping for input frequencies f=0 to 23 for a) $f_{s1} = 10$ and b) $f_{s1} = 11$. 19

4.1 Block diagram of a two channel receiver architecture to determine a single frequency f 22

5.1 Block diagram of a three channel receiver architecture to determine a single frequency f 26

6.1 DFT for two unknown frequencies for a) $f_{s1} = 10$ and b) $f_{s2} = 11$. . . 28

6.2 Normalized DFT for two unknown frequencies for a) $f_{s1} = 10$ and b) $f_{s2} = 11$. 29

7.1 Normalized DFT for frequencies from 0 to 10 for a) $f_{s1} = 10$ and b) $f_{s2} = 11$. 34

7.2 Frequency components and amplitudes: a) actual and b) calculated . 35

8.1 Normalized DFT components at $f_{s1} = 10$ Hz: a) real component and b) imaginary component. 41

8.2 Normalized DFT components at $f_{s2} = 11$ Hz: a) real component and b) imaginary component. 42

9.1 Channel architecture to resolve an undersampled signal utilizing a single sampling frequency 51

10.1 Normalized DFT of sinusoid at $f = 2.3153$ Hz: a) real component for $f_{s1} = 10$ Hz, b) imaginary component for $f_{s1} = 10$ Hz, c) real component for $f_{s2} = 11$ Hz, and d) imaginary component for $f_{s2} = 11$ Hz. 57

10.2 Spectrum calculated for single frequency at 2.3153 Hz: a) real component and b) imaginary component 58

10.3 Spectra of a signal with frequency components from 0 to 10 Hz in 1/2 Hz increments: a) real component of sampled bandlimited signal, b) imaginary component of bandlimited signal, c) real component of sampled original signal, and d) imaginary component of original signal 59

10.4 Spectra of a signal with frequency components from 0 to 10 Hz in 1/2 Hz increments: a) calculated real component, b) calculated imaginary component, c) actual real component, and d) actual imaginary component. 60

10.5 Normalized DFT with 0.01 Hz resolution of sinusoid at $f = 2.3153$ Hz: a) real component fo $f_{s1} = 10$ Hz, b) imaginary component for $f_{s1} = 10$ Hz, c) real component for $f_{s2} = 11$ Hz, and d) imaginary component for $f_{s2} = 11$ Hz. 61

ACKNOWLEDGMENT

Sir Isaac Newton once attributed his achievements to those great men who had gone before him by saying he was "...standing on the shoulders of giants." I have felt the same way during my studies at the Naval Postgraduate School and particularly during the thesis process. I would like to especially thank Professor Phillip E. Pace for the tremendous encouragement and support he has given me during my thesis preperation. He not only conceived the original direction for my thesis but was invaluable in its formulation and presentation.

I would also like to thank Professor David Styer of the University of Cincinnati. The chapter on the Symmetrical Number System would not have been possible without him nor would I understand much of the math in the thesis. Collectively I would like to thank both him and Professor Pace for teaching me so much during research on my thesis topic. I had the pleasure of co-authoring two papers with them and learned more during that process than at any other time during my education at the Naval Postgraduate School.

I would like to thank my wife, Sonya for her constant love and support in all things. She is the most patient and understanding person I know and all success would be hollow without her by my side. A longtime bachelor, I thought I was a happy man until I met Sonya and she taught me what true happiness was.

Lastly, I would like to thank my Lord and Saviour Jesus Christ without Whom life would be meaningless. I thank Him for my life and for the many gifts and talents I have been so undeservedly blessed with.

This research was supported by the Space and Naval Warfare Systems Command PMW-178.

I. INTRODUCTION

A. BACKGROUND

For a periodic discrete signal $x_p(nT)$ with a period of N samples or a discrete signal $x(nT)$ that contains exactly N samples, a transform known as the discrete Fourier transform (DFT) is defined. The DFT transforms the N time-domain samples to N frequency-domain coefficients where the frequencies are $2\pi k/NT$ where $k = 0, 1, \ldots, N-1$ and T is the sampling period. The DFT coefficients $X(k)$ are also periodic with period N. For actual computations using a digital computer, the continuous signal is digitized, the number of samples is limited, and the Fourier representation is obtained for a finite number of frequency values. The digitization of the signal is usually governed by the Nyquist criterion where it is assumed that the input signal must be bandlimited ($0 \leq f \leq f_s/2$) before going into the analog-to-digital converter (ADC). The Nyquist theorem however, only places a limitation on the information that can be derived from a single set of digitized data [3]. That is, a single set of digitized data limits subsequent analysis to an $f_s/2$ bandwidth unless there is additional information available. With additional information, the frequency components $f > f_s/2$, which appear ambiguously due to undersampling, may be resolved provided they are within the dynamic range of the algorithm utilized.

B. UNDERSAMPLING

There are several advantages to an undersampled system [4]. Among these are a reduction in the speed requirements on the digital section of the system, a relaxation on the analog anti-aliasing filter requirements, and the possibility of extending the capabilities of existing systems with relatively minor redesign. Also, a good deal of power and money can be saved in the analog-to-digital converter section. The

main problem in identifying the frequencies present in an undersampled signal is the resolution of the ambiguities.

There has been a great deal of research investigating methods to either detect aliasing or to recover undersampled signals. Baier and Furst [1] have proposed a method to *detect* aliased frequency components by utilizing two ADC's at slightly different sampling rates. The frequency components occuring in the resulting spectra are also slighty shifted and the difference in the two spectra allows for detection of the aliased frequency component. Barbarossa [2] has proposed a method which can recover an undersampled signal using time-frequency domain analysis and computing the Wigner-Ville distribution of the signal. Rader [10] has described an undersampling technique that can recover periodic signals by reconstructing the waveform using a set of *trial* sampling periods. The trial period which yields the waveform of smallest variation is then considered to be the correct period and the resulting waveform the correct waveform. Zoltowski and Matthews [13] have devised an algorithm for unambiguous estimation of both frequency and phase for a single frequency utilizing eigenvector information. To come more in line with real-time wideband processing, methods based on the use of phase shift information to resolve the ambiguities in a single frequency undersampled signal have also been investigated [12], [11]. Finally, Martin and Rasmussen [6] have proposed a testbed for evaluating the impact that ADC imperfections would have towards limiting digital implementations of undersampling.

C. PRINCIPLE CONTRIBUTION

Current research in the area of undersampling is limited in two principal ways. First, while methods exist that can unambiguously detect a single frequency, none of the research proposes a dynamic range to its system or algorithm for detection.

Secondly, no algorithm currently exists which allows for the unambiguous detection of a signal containing a spectrum of undersampled frequencies.

The principal contribution of this thesis is to resolve both problems. This thesis presents algorithms which solve for an undersampled spectrum of frequencies. The algorithms are based upon the mathematical properties of the Symmetrical Number System (SNS) [9] and the relationship between digital signals and the SNS. Each of the algorithms developed are simple linear solutions with dynamic ranges which ensure no ambiguity in the resolved spectrum.

D. THESIS OUTLINE

This thesis presents two algorithms which unambiguously resolve an undersampled spectrum band-limited beyond Nyquist. For the first algorithm, it will first be shown that if a signal is sampled at two different sampling frequencies and the DFT is applied and normalized, two unique spectra result. Utilizing the bin and amplitude information of each spectrum as well as knowledge of how the real and imaginary frequency components alias into DFT bins, it is shown that the original frequency components may be unambiguously resolved utilizing a matrix multiplication. For the second algorithm, it will be shown that if both the signal and a band-limited version of the signal are processed, it is possible to resolve a spectrum of frequencies up to nearly twice the Nyquist rate. The band-limited version of the signal allows for the unambiguous resolution of frequencies below $\frac{f_s}{2}$ which is then applied to solve for frequencies $\frac{f_s}{2} < f \leq f_s - 1$

Since the properties of the SNS are what the solution methods utimately utilize, Chapter II begins with a detailed look at the Symmetrical Number System (SNS) and its dynamic range for unambiguously detecting a tone frequency is introduced and proven. Chapter III shows that the DFT encodes frequency information in a

format that is exactly the same as the SNS which means that a digital sequence has the same properties as the SNS. Beginning to resolve undersampled frequencies, the properties of the SNS allow us to develop the architectures of Chapters IV and V, in which two and three channel architectures are introduced which unambiguously resolve a single frequency within the SNS dynamic range. Moving towards resolving multiple frequencies, Chapter VI shows that the DFT can be normalized and using the properties of the SNS, a method is demonstrated which resolves two undersampled frequencies in a signal. With the SNS and normalization, there is now sufficient information of resolve an entire spectrum of frequencies. In Chapter VII the bin locations and normalized amplitudes are used to set up linear equations which solve for an undersampled spectrum with frequencies with zero-phase and no DFT leakage. Since real world signals have random phase, Chapter VIII removes the phase constraint and utlimately presents the first algorithm which resolves frequencies with random phase and no DFT leakage and band-limited at twice Nyquist. Chapter IX presents the second algorithm which requires only one sampling frequency but has the same dynamice range as the first algorithm. Finally, in Chapter X, the limitations of the two algorithms are explored and a possible direction for resolving the limitation is explored.

II. THE SYMMETRICAL NUMBER SYSTEM

A. DEFINING THE SNS WAVEFORM

In the SNS preprocessing, r different periodic symmetrical waveforms are used with periods based on r different, pairwise relatively prime, integer lengths $m_1, m_2, \ldots, m_r$. For each integer, k, an r dimensional column vector A_k is formed by placing the value of the i^{th} waveform at k in the i^{th} position, $1 \leq i \leq r$. It is then desired to find out the largest set of vectors $A_0, A_1, \ldots, A_k$ that are distinct. This sequence of $k+1$ vectors forms the unambiguous output of the system. This number, $k+1$, is called the *dynamic range* of the system. Dynamic range refers to the fact that each vector up to A_k is unique in the same way that frequencies up to $f_s/2$ are unique and unambiguous when sampled and conventional methods are applied.

The definition of the SNS waveform is given below.

Definition 2.1 *Let m be an integer greater than 1. For an integer h such that $0 \leq h < m$, define*

$$a_h = \min\{h, m-h\} \ . \tag{1}$$

This function is extended periodically with period m. That is,

$$a_{h+nm} = a_h \tag{2}$$

where $n \in \{0, \pm 1, \pm 2, \ldots\}$, and a_h is called a symmetrical residue of $h + nm$ modulo m.

Let $\overline{a}_m$ be the row vector $[a_0, a_1, \ldots, a_{m-1}]$. For m odd

$$\overline{a}_m = \left[0, 1, \ldots, \left\lfloor \frac{m}{2} \right\rfloor, \left\lfloor \frac{m}{2} \right\rfloor, \ldots, 2, 1\right] \tag{3}$$

where $\lfloor x \rfloor$ indicates the greatest integer less than or equal to x. For m even,

$$\overline{a}_m = \left[0, 1, \ldots, \frac{m}{2}, \frac{m}{2} - 1, \ldots, 2, 1\right] \ . \tag{4}$$

Both have size $1 \times m$ and consist of the symmetrical residues elements a_h, $0 \leq h < m$. This shows the form of one period of length m. From this definition it is emphasized that it follows for any integers, h, k, $a_h = a_{h+k}$ if and only if $h \equiv \pm(h+k) (\text{mod } m)$.

B. DYNAMIC RANGE OF AN SNS SYSTEM

Having introduced the SNS waveform, it is useful to introduce the dynamic range of an SNS system given its moduli.

Theorem 2.1 *Let $m_1, \ldots, m_r$ be r pairwise relatively prime moduli, and let A_0, A_1, $A_2, \ldots$ be vectors formed by the symmetrical number system given in Definition 2.1.*

a) If one of the moduli (m_1) is even, then the dynamic range of the system is

$$\hat{M} = \min \left\{ \frac{m_1}{2} \prod_{\ell=2}^{j} m_{i_\ell} + \prod_{\ell=j+1}^{r} m_{i_\ell} \right\} \tag{5}$$

where j ranges from 1 to $r-1$ and $m_{i_2}, m_{i_3}, \ldots, m_{i_r}$ range over all permutations of $\{2, 3, \ldots, r\}$.

b) If all of the moduli are odd, then the dynamic range of the system is

$$\hat{M} = \min \left\{ \frac{1}{2} \prod_{\ell=1}^{j} m_{i_\ell} + \frac{1}{2} \prod_{\ell=j+1}^{r} m_{i_\ell} \right\}, \tag{6}$$

where j ranges from 1 to $r-1$ and $m_{i_1}, m_{i_2}, \ldots, m_{i_r}$ range over all permutations of $\{1, 2, \ldots, r\}$.

1. Example of the SNS Dynamic Range

Let $m_1 = 4$, $m_2 = 3$, and $m_3 = 5$. We must minimize the set of values:

$$\left\{ \frac{m_1}{2} + m_2 \cdot m_3, \ \frac{m_1}{2} m_2 + m_3, \ \frac{m_1}{2} m_3 + m_2 \right\} = \{17, \ 11, \ 13\}.$$

The dynamic range is the minimum value of this set, 11, as is verified in Table 2.1. We see that $A_{11} = A_1$, and A_{11} is the first repetitive vector. In other

	0	1	2	3	4	5	6	7	8	9	10	11	12	13	$\cdots$
m_1	0	1	2	1	0	1	2	1	0	1	2	1	0	1	$\cdots$
m_2	0	1	1	0	1	1	0	1	1	0	1	1	0	1	$\cdots$
m_3	0	1	2	2	1	0	1	2	2	1	0	1	2	2	$\cdots$

Table 2.1: Integer Values for the $m_1 = 4$, $m_2 = 3$, and $m_3 = 5$

words, $A_0, \ldots, A_{10}$ is a set of 11 distinct vectors and, $A_0, \ldots, A_{11}$ is not a set of distinct vectors. This shows directly that the dynamic range of this system is 11. A repeated vector is called an *ambiguity* of the system. In the above example A_{11} is the first ambiguity of the system.

C. PROOF OF THE SNS DYNAMIC RANGE

Before starting the proof of Theorem 2.1 it is necessary to express the general idea that will be used. Suppose that $m_1, \ldots, m_r$ are r positive pairwise relatively prime integers. Also suppose that

$$A_h = \begin{bmatrix} a_h^1 \\ a_h^2 \\ \vdots \\ a_h^r \end{bmatrix} = \begin{bmatrix} a_{h+k}^1 \\ a_{h+k}^2 \\ \vdots \\ a_{h+k}^r \end{bmatrix} = A_{h+k} \tag{7}$$

so that there is an ambiguity at the position $h+k$ (since the vector is indistinguishable from that at position h), where $h \geq 0$ and $k \geq 1$.

The key to the proof is that fact that $A_h = A_{h+k}$ if an only if $h \equiv \pm(h + k) \pmod{m_i}$ for $1 \leq i \leq r$. Thus the proof involves systems of linear congruences and the Chinese Remainder Theorem [7]. The goal is to find the least value of $h + k$ that is an ambiguity. In general all permutations of subscripts $1, 2, \ldots, r$ must be worked, but for the sake of a clearer presentation the subscripts are not permuted.

1. Proof of Theorem 2.1a.

Let $m_1 = 2m$ be even.

Case I:

$$h \equiv (h+k) \pmod{m_i}, \qquad 1 \le i \le j \quad (\le r) \tag{8}$$

$$h \equiv -(h+k) \pmod{m_i}, \qquad j+1 \le i \le r \tag{9}$$

Case II:

$$h \equiv -(h+k) \pmod{m_i}, \qquad 1 \le i \le j \tag{10}$$

$$h \equiv (h+k) \pmod{m_i}, \qquad j+1 \le i \le r \tag{11}$$

Note that the two cases are opposite in terms of the plus or minus signs in the congruences. These would not be separate cases except for the fact that m_1 is the even modulus.

a. Case I

Suppose congruences (8) and (9) are true, i.e., $k \equiv 0 \pmod{m_i}$ for $1 \le i \le j$. Since the moduli are relatively prime in pairs, $k \equiv 0 \pmod{\prod_{i=1}^{j} m_i}$. Note that k is even since m_1 is even. It follows that $k = a \prod_{i=1}^{j} m_i$ for some $a \in \{1, 2, \ldots\}$ so

$$\frac{k}{2} = am \prod_{i=2}^{j} m_i \, . \tag{12}$$

Continuing on for the moduli m_i, the condition $i \ge j+1$ is examined next. From (9)

$$h \equiv -\frac{k}{2} \pmod{m_i} \tag{13}$$

for $j+1 \le i \le r$. Since these m_i are pairwise relatively prime, the Chinese remainder theorem guarantees that there is a unique solution $h \pmod{\prod_{i=j+1}^{r} m_i}$ to this system. Therefore, there will be exactly $\prod_{i=1}^{j} m_i$ solutions $\pmod{\prod_{i=1}^{r} m_i}$. Let b' be the least integer such that

$$b' \prod_{i=j+1}^{r} m_i - \frac{k}{2} \ge 0 \, . \tag{14}$$

Note that if we set

$$h_1 = b' \prod_{i=j+1}^{r} m_i - \frac{k}{2}\,, \tag{15}$$

then

$$0 \leq h_1 < \prod_{i=j+1}^{r} m_i \tag{16}$$

and

$$h_1 \equiv -\frac{k}{2} \pmod{m_i} \tag{17}$$

for $j+1 \leq i \leq r$. This h_1 is *the* solution (mod $\prod_{i=j+1}^{r} m_i$). All solutions (mod $\prod_{i=1}^{r} m_i$) are of the form

$$h = h_1 + \tilde{b} \prod_{i=j+1}^{r} m_i \tag{18}$$

for $0 \leq \tilde{b} < \prod_{i=1}^{j} m_i$. Using (15) the ambiguities, $h + k$, will have the form

$$h + k = h_1 + \tilde{b} \prod_{i=j+1}^{r} m_i + k = b' \prod_{i=j+1}^{r} m_i + \tilde{b} \prod_{i=j+1}^{r} m_i + \frac{k}{2} \tag{19}$$

Using (12)

$$h + k = am \prod_{i=2}^{j} m_i + b \prod_{i=j+1}^{r} m_i \tag{20}$$

where $b = b' + \tilde{b} \in \{1, 2, \ldots\}$ and $a \in \{1, 2, \ldots\}$.

b. Case II

Although the particulars of this case are different from those of Case I, the line of argument is the same, and the result is exactly the same:

$$h + k = am \prod_{i=2}^{j} m_i + b \prod_{i=j+1}^{r} m_i \tag{21}$$

where a and b are positive integers.

Now the two cases have been treated and it is evident that all the ambiguous values $h+k$, have the form (20) or (21) and these forms are indistinguishable. The least number of this form (or the first of many ambiguities) is found by setting

$a = b = 1$. Next it is shown that

$$m \prod_{i=2}^{j} m_i + \prod_{i=j+1}^{r} m_i \tag{22}$$

is one of the ambiguities.

Suppose

$$m \prod_{i=2}^{j} m_i < \prod_{i=j+1}^{r} m_i \ . \tag{23}$$

We revert to Case I and set $a = 1$ in (12) so

$$\frac{k}{2} = m \prod_{i=2}^{j} m_i \tag{24}$$

Then, in (14) $b' = 1$, so

$$h_1 = \prod_{i=j+1}^{r} m_i - \frac{k}{2} \tag{25}$$

and

$$h_1 + k = m \prod_{i=2}^{j} m_i + \prod_{i=j+1}^{r} m_i \tag{26}$$

is an ambiguity. That is, the vector corresponding to h_1 is the same as the vector corresponding to $h_1 + k$.

The alternative is that

$$\prod_{i=j+1}^{r} m_i < m \prod_{i=2}^{j} m_i \ . \tag{27}$$

Now we use Case II with $a = b = 1$. We can set

$$\frac{k}{2} = \prod_{i=j+1}^{r} m_i \ . \tag{28}$$

Then

$$h_1 = m \prod_{i=2}^{j} m_i - \frac{k}{2} \tag{29}$$

is positive, and

$$h_1 + k = m \prod_{i=2}^{j} m_i + \prod_{i=j+1}^{r} m_i \tag{30}$$

is an ambiguity.

Recall that

$$\begin{bmatrix} a_h^1 \\ a_h^2 \\ \vdots \\ a_h^r \end{bmatrix} = \begin{bmatrix} a_{h+k}^1 \\ a_{h+k}^2 \\ \vdots \\ a_{h+k}^r \end{bmatrix} \tag{31}$$

if and only if $h \equiv \pm(h+k) \pmod{m_i}$, $i = 1, \ldots, r$. There are 2^n possibilities for choice of plus or minus signs in these congruences. For j fixed we have looked at two possibilities and found the minimum ambiguity. All others can be found by varying j and by permuting the order of the moduli. Thus

$$\hat{M} = \min \left\{ m \prod_{l=2}^{j} m_{i_l} + \prod_{l=j+1}^{r} m_{i_l} \right\} \tag{32}$$

is the minimum ambiguity.

2. Proof of Theorem 2.1b.

Let $m_1, \ldots, m_r$ be r odd pairwise relatively prime natural numbers. Recall that

$$\begin{bmatrix} a_h^1 \\ a_h^2 \\ \vdots \\ a_h^r \end{bmatrix} = \begin{bmatrix} a_{h+k}^1 \\ a_{h+k}^2 \\ \vdots \\ a_{h+k}^r \end{bmatrix} \tag{33}$$

if and only if $h \equiv \pm(h+k) \pmod{m_i}$ for $1 \leq i \leq r$. Suppose $h \equiv (h+k) \pmod{m_i}$ for $1 \leq i \leq j$ and $h \equiv -(h+k) \pmod{m_i}$ for $j+1 \leq i \leq r$. The first set of congruences implies that $k \equiv 0 \pmod{m_i}$, $1 \leq i \leq j$. Thus

$$k = a \prod_{i=1}^{j} m_i \tag{34}$$

for $a \in \{1, 2, \ldots\}$. The second set of congruences implies that $2h \equiv -k \pmod{m_i}$ i.e.,

$$h \equiv \frac{m_i - 1}{2} k \pmod{m_i} \tag{35}$$

for $j+1 \leq i \leq r$. Again the proof is split into two cases, this time depending on whether k is even or odd.

a. Case I

Suppose k even. Then

$$h \equiv -\frac{k}{2} \pmod{m_i} \tag{36}$$

for $j+1 \leq i \leq r$. Let b' be the least integer such that

$$h_1 = b' \prod_{i=j+1}^{r} m_i - \frac{k}{2} \geq 0 \tag{37}$$

Note $b' \in \{1, 2 \ldots\}$. This is the unique solution (mod $\prod_{i=j+1}^{r} m_i$) to the set of congruences (36). Every solution to the original problem is of the form

$$h = b' \prod_{i=j+1}^{r} m_i + \tilde{b} \prod_{i=j+1}^{r} m_i - \frac{k}{2} \tag{38}$$

where

$$0 \leq \tilde{b} < \prod_{i=1}^{j} m_i \, . \tag{39}$$

By (34) and (38), all ambiguities $h + k$ that arise from these values of h are of the form

$$h + k = \frac{a}{2} \prod_{i=1}^{j} m_i + \frac{b}{2} \prod_{i=j+1}^{r} m_i \tag{40}$$

where $b = 2(b' + \tilde{b})$ is an even positive integer. Note that k is even if and only if a is even.

b. Case II

Suppose that k is odd. As in Case I, all ambiguities $h + k$ that arise from these values of h are of the form

$$h + k = \frac{a}{2} \prod_{i=1}^{j} m_i + \frac{b}{2} \prod_{i=j+1}^{r} m_i \tag{41}$$

where a and b are odd positive integers.

Combining Cases I and II, note that the smallest value of (40), (41) is found when $a = b = 1$. Furthermore, when $a = b = 1$, and $\prod_{i=1}^{j} m_i < \prod_{i=j+1}^{r} m_i$ this

is an ambiguity: Let

$$h = \frac{1}{2}\prod_{i=j+1}^{r} m_i - \frac{1}{2}\prod_{i=1}^{j} m_i \tag{42}$$

and $k = \prod_{i=1}^{j} m_i$. It is easily checked that $h \equiv h + k(mod\ \ m_i)$ for $1 \leq i \leq j$ and $h \equiv -(h+k) \pmod{m_i}$ for $j+1 \leq i \leq r$. When $\prod_{i=j+1}^{r} m_i < \prod_{i=1}^{i} m_i$ we must solve the permuted problem: $h \equiv h+k \pmod{m_i}$ for $j+1 \leq i \leq r$ and $h \equiv -(h+k) \pmod{m_i}$ for $1 \leq i \leq j$. This time $k = \prod_{i=j+1}^{r} m_i$, and $h = (1/2)\prod_{i=1}^{i} m_i - (1/2)\prod_{i=j+1}^{r} m_i$ give the ambiguity at $h+k$. Since the solution to the problem involves looking at all permutations this gives the minimum ambiguity. This completes the proof of Theorem 2.1b.

Theorem 2.1 provides the basis for predicting the dynamic range of any system which encodes information in a format identical to the SNS. In fact, in the next chapter it is shown that the process of digital sampling encodes frequency information into the SNS format which allows the DFT to be treated identically to the SNS.

III. DFT AND SNS RELATIONSHIP

A. DIGITAL SAMPLING AND ALIASING

Consider a single frequency signal sampled at two different sampling frequencies. Digital uniform sampling of an analog waveform with frequency f produces a discrete waveform which is symmetrical about the sampling frequency, $f_s/2$. Assume for this system that the two sampling frequencies are $f_{s1} = 10$ and $f_{s2} = 11$. After sampling, an analog input signal, $x(t)$, becomes a discrete sequence, $x(nT)$. This periodic sequence has a digital frequency given by $\omega = 2\pi(f/f_s)$. A signal with digital frequency $0 \leq \omega \leq \pi$ is indistinguishable from a signal with digital frequency $n\pi \leq \omega \leq (n+1)\pi$, $n = 1, 2, 3, \ldots$, an effect known as aliasing.

B. DIGITAL FREQUENCY MAPPING

The digital frequency of a sampled sinusoid can be mapped into the z-domain as shown in Figure 3.1a. For simplicity assume a sinusoid $x(t) = 2\cos 2\pi ft$ and after sampling

$$x(n) = 2\cos\omega n = e^{j\omega n} + e^{-j\omega n} \,. \tag{43}$$

If $f = f_s/4$, this corresponds to $\omega = \pi/2$. If $f = f_s/2$, $\omega = \pi$. Since the signal is real, the signal appears in complex conjugate pairs on the z-plane. For frequencies between $f_s/2$ and f_s, the frequencies map back to their conjugate on the upper half of the complex plane. If the frequency is increased beyond f_s, a full trip is made around the unit circle and the mapping repeats. Figure 3.1b illustrates the mapping with each triangle representing a full rotation around the unit circle in the z-plane. The abscissa represents the input analog frequency while the ordinate represents the digital frequency mapping. Note that an infinite number of analog frequencies will map into each digital frequency $0 \leq \omega \leq \pi$.

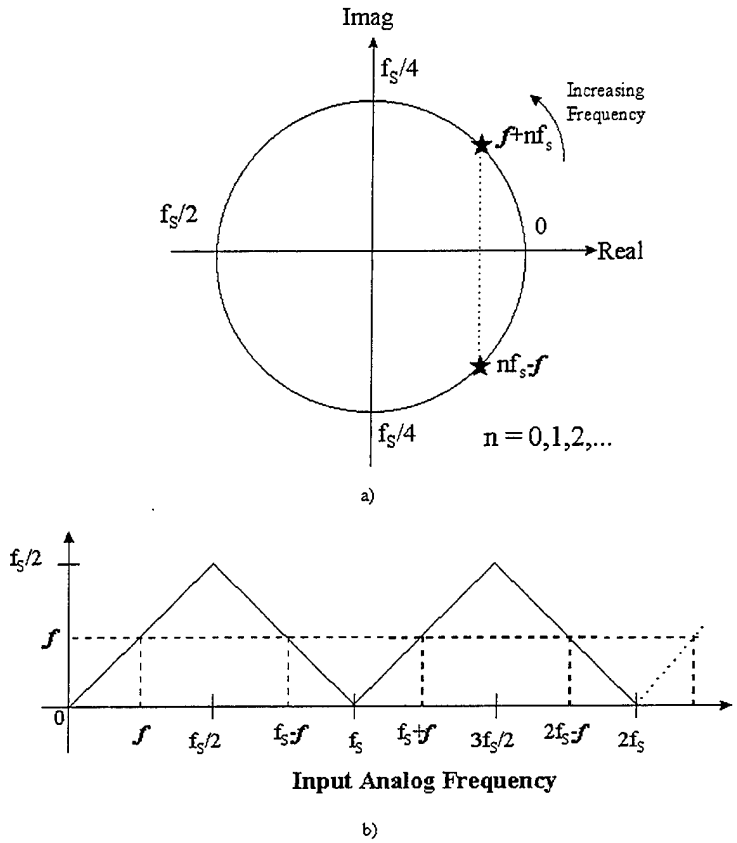

Figure 3.1: a)Z-plane mapping of an input analog signal. b) sampled frequency output.

C. DFT BINS AND THE SNS

Recall that the DFT is given by:

$$X(k) = \sum_{n=0}^{N-1} x(n) e^{-j(2\pi nk/N)} \qquad k = 0, \ldots, N-1 \; . \tag{44}$$

Application of the DFT to $x(n)$ yields a discrete spectrum where $X(k)$ is the energy contained in the signal at each digital frequency $\omega = 2\pi k/N$. The discrete spectrum $X(k)$ has N indices with the digital frequency of each index given by:

$$\left[0,\, 2\pi\frac{1}{N}, \cdots, 2\pi\frac{(N/2)}{N},\, 2\pi\frac{(N/2+1)}{N}, \cdots,\, 2\pi\frac{(N-2)}{N},\, 2\pi\frac{(N-1)}{N}\right] \quad \text{for } N \text{ even} \; , \tag{45}$$

and

$$\left[0,\ 2\pi\frac{1}{N},\cdots,2\pi\frac{(N-1)/2}{N},\ 2\pi\frac{(N+1)/2}{N},\cdots,\ 2\pi\frac{(N-2)}{N},\ 2\pi\frac{(N-1)}{N}\right] \quad \text{for } N \text{ odd}. \tag{46}$$

The analog frequency corresponding to each index is obtained by multiplying each value by f_s. Since signals with digital frequencies in the range $\pi < \omega < 2\pi$ are indistinguishable from signals with digital frequencies $0 \leq \omega \leq \pi$, the digital frequency of each index can also be written as:

$$\left[0,\ 2\pi\frac{1}{N},\cdots,\ 2\pi\frac{(N/2)}{N},\ 2\pi\frac{(N/2-1)}{N},\cdots,\ 2\pi\frac{2}{N},\ 2\pi\frac{1}{N}\right] \quad \text{for } N \text{ even}, \tag{47}$$

and

$$\left[0,\ 2\pi\frac{1}{N},\cdots,\ 2\pi\frac{\lfloor N/2\rfloor}{N},\ 2\pi\frac{\lfloor N/2\rfloor}{N},\cdots,\ 2\pi\frac{2}{N},\ 2\pi\frac{1}{N}\right] \quad \text{for } N \text{ odd}, \tag{48}$$

where $\lfloor x \rfloor$ represents the greatest integer less than or equal to x. More simply, the spectrum $X(k)$ resolves into N integer indices and incoming signals will map into unique bins:

$$\left[0,1,\cdots,\frac{N}{2},\frac{N}{2}-1,\cdots,2,1\right] \quad \text{for } N \text{ even}, \tag{49}$$

and

$$\left[0,1,\cdots,\lfloor\frac{N}{2}\rfloor,\lfloor\frac{N}{2}\rfloor,\cdots,2,1\right] \quad \text{for } N \text{ odd}. \tag{50}$$

That is, since frequency indices greater than $N/2$ are redundant for real signals, the highest unaliased frequency that can be observed corresponds to the $N/2$ index. From the above discussion, it is clear that the DFT maps real signals naturally into the symmetrical number system [9]. In this case, the modulus described in [9] and in Chapter II is the sampling frequency, f_s. The number of indices N is given by $N = f_s T_L$, where T_L is the total sampling time.

D. ILLUSTRATING THE RELATIONSHIP

Figure 3.2 illustrates the DFT mapping for two channels where $f_{s1} = 10$ and

$f_{s2} = 11$ for input frequencies $f = 0$ to 23. In this case, $T_L = 1$ so $N_1 = 10$ and $N_2 = 11$. In the figure, the abscissa corresponds to the incoming frequency while the ordinate corresponds to the bin the signal is resolved into. Table 3.1 displays the input frequency and the resulting DFT bin for each sampling frequency. Note that frequencies resolve as described in (49) and (50). By considering both channels, it is possible to unambiguously resolve signal frequencies in the dynamic range determined by the SNS, $(0 \leq f \leq 15)$.

Simply knowing that the DFT is in the SNS format and what the dynamic range is for any given sampling frequencies would be useless unless the information can be used to resolve undersampled frequencies within the dynamic range. The next two chapters detail two and three channel architectures as well as solution methods which will resolve a single undersampled frequency band-limited within the dynamic range of the SNS system.

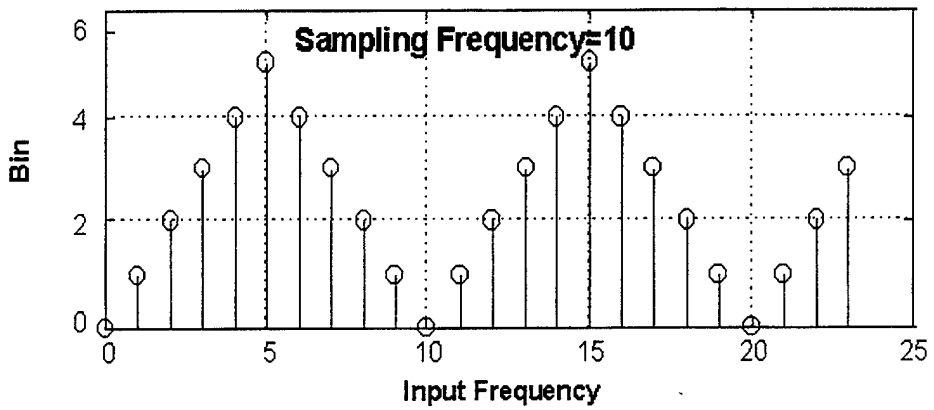

a)

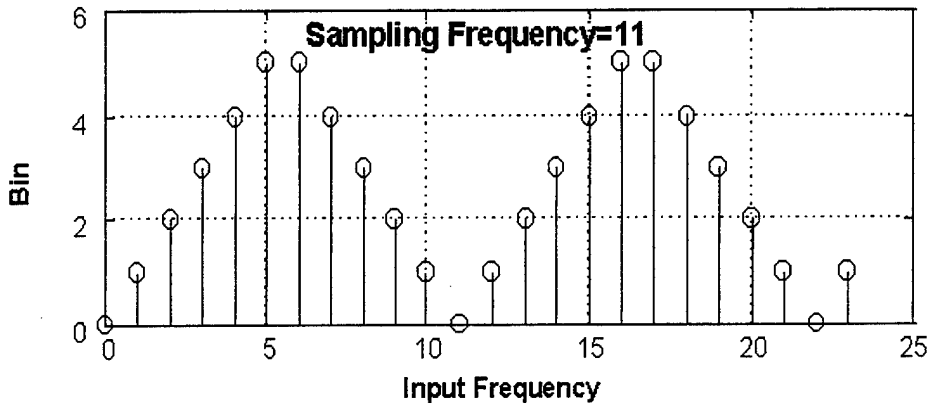

b)

Figure 3.2: a)DFT mapping for input frequencies f=0 to 23 for a) $f_{s1} = 10$ and b) $f_{s1} = 11$.

Input Frequency	DFT Bins	
f	$f_s = 10$	$f_s = 11$
0	0	0
1	1	1
2	2	2
3	3	3
4	4	4
5	5	5
6	4	5
7	3	4
8	2	3
9	1	2
10	0	1
11	1	0
12	2	1
13	3	2
14	4	3
15	5	4
16	4	5
17	3	5
18	2	4
19	1	3
20	0	2
21	1	1
22	2	0
23	3	1

Table 3.1: Input Frequency and Resulting DFT Bins for 2 Channel Example

IV. RESOLVING THE TWO CHANNEL CASE

A. THE GENERAL SETUP

Figure 4.1 shows the block diagram of a two-channel receiver architecture to determine a single frequency f. In this architecture the ADC sampling frequencies f_{s1} and f_{s2} are relatively prime. The DFT outputs are thresholded to detect the frequency bins. The frequency bins a_1 and a_2 are then used by the SNS-to-decimal algorithm to determine the frequency of the input signal. Let $m_1 = f_{s1}$ and $m_2 = f_{s2}$ and suppose that the incoming frequency, f (unknown) lies within the dynamic range $\hat{M}$ of the SNS system (5), (6). Thus, $f \equiv \pm a_1 (\text{mod } m_1)$ and $f \equiv \pm a_2 (\text{mod } m_2)$. For each of these congruences either the plus or the minus is correct, but it is not known which. Thus, there are four sets of two equations:

$$\begin{aligned}
&\text{i)} && f \equiv a_1 (\text{mod } m_1), \\
& && f \equiv a_2 (\text{mod } m_2), \\
&\text{ii)} && f \equiv a_1 (\text{mod } m_1), \\
& && f \equiv -a_2 (\text{mod } m_2), \\
&\text{iii)} && f \equiv -a_1 (\text{mod } m_1), \\
& && f \equiv -a_2 (\text{mod } m_2), \\
&\text{iv)} && f \equiv -a_1 (\text{mod } m_1), \\
& && f \equiv a_2 (\text{mod } m_2) \ .
\end{aligned}$$

The Chinese remainder theorem [7] guarantees that each of these has a unique solution modulo $m_1 m_2$, and Theorem 2.1 guarantees that exactly one of these solutions lies within the dynamic range of the system and this is the value of f. In fact, it is only necessary to solve i) and ii), at most, because the solutions to iii) and iv) are the negatives of the solutions to i) and ii), respectively.

Recall that in the standard statement of the Chinese remainder theorem we wish to solve for f, where $f \equiv a_i (\text{mod } m_i)$, $1 \leq i \leq r$, and the m_i are pairwise

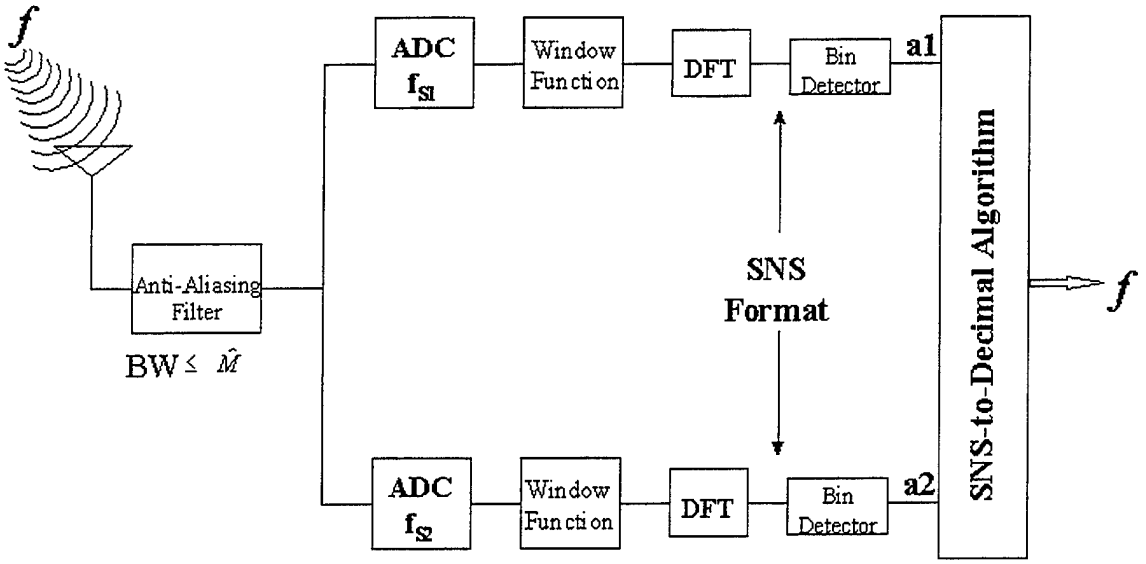

Figure 4.1: Block diagram of a two channel receiver architecture to determine a single frequency f

relatively prime. The theorem states that there is a unique solution modulo $M = m_1 m_2 \cdots m_r$. A standard method of solution is to find integers b_i such that

$$\frac{M b_i}{m_i} \equiv 1 (\text{mod } m_i) \ , \tag{51}$$

$i = 1, 2, \cdots, r$, in which case the solution

$$f \equiv M b_1 a_1 / m_1 + M b_2 a_2 / m_2 + \cdots + M b_r a_r / m_r (\text{mod } M) \ . \tag{52}$$

Returning to the two channel case, note that the values of b_1 and b_2 depend only on m_1 and m_2, and not at all on $\pm a_1$ or $\pm a_2$. Thus it may be assumed that the constants $c_1 = m_2 b_1 (= M b_1 / m_1)$ and $c_2 = m_1 b_2$ are known, and that the SNS-to-decimal algorithm only needs to evaluate $\pm c_1 a_1 \pm c_2 a_2$ modulo $M (= m_1 m_2)$, and pick the one value that lies within the dynamic range.

B. SET-UP FOR A PARTICULAR TWO CHANNEL RECEIVER

Let $m_1 = 330$ and $m_2 = 337$. Then

$$b_1 = -47 \quad \text{solves} \quad 337b_1 \equiv 1 \pmod{330}\,, \tag{53}$$

and

$$b_2 = 48 \quad \text{solves} \quad 330b_2 \equiv 1 \pmod{337}\,. \tag{54}$$

Thus, $c_1 = m_2 b_1 = -15,839$, and $c_2 = m_1 b_2 = 15,840$. Also, $M = 111,210$, and, by Theorem 2.1, the dynamic range of the system is $m_1/2 + m_2 = 502$. These coefficients are hardwired and do not need to be recomputed.

C. SOLVING A PARTICULAR CASE - THE WORK OF THE ALGORITHM

Suppose that the frequency of the incoming signal is f, $0 \leq f \leq 501$, and $a_1 = 59$ and $a_2 = 66$. By Theorem 2.1, f is the unique solution to $\pm(-15,839)(59) \pm (15,840)(66)$ modulo $111,210$ that lies in the interval $[0, 501]$. First try $(-15,839) \cdot 59 + 15,840 \cdot 66 = 110,939$; this is congruent to -271 modulo 111,210, so case iii) solves $f = 271$.

It is emphasized that this is the only computation the algorithm needs to compute.

D. SPECIAL CASES

In special cases there are even quicker solutions than given in section C. For example, suppose $m_1 = 2p$ and $m_2 = 2p + 1$. By Theorem 2.1 the dynamic range of the system is $m_1/2 + m_2 = 3p + 1$. Frequencies within the dynamic range will fall into bins as follows:

$$\underbrace{\begin{bmatrix} 0 \\ 0 \end{bmatrix}\begin{bmatrix} 1 \\ 1 \end{bmatrix}\cdots\begin{bmatrix} p \\ p \end{bmatrix}}_{p+1 \text{ terms}}\underbrace{\begin{bmatrix} p-1 \\ p \end{bmatrix}\begin{bmatrix} p-2 \\ p-1 \end{bmatrix}\cdots\begin{bmatrix} 0 \\ 1 \end{bmatrix}}_{p \text{ terms}}\underbrace{\begin{bmatrix} 1 \\ 0 \end{bmatrix}\begin{bmatrix} 2 \\ 1 \end{bmatrix}\cdots\begin{bmatrix} p \\ p-1 \end{bmatrix}}_{p \text{ terms}} \tag{55}$$

The top bin represents the sampling frequency of $m_1 = 2p$ and the bottom $m_2 = 2p+1$. Now suppose the incoming frequency, f, is resolved into bins a_1 and a_2, respectively. From the above it is clear that:

$$f = \begin{cases} a_1 & \text{if } a_1 = a_2 \\ m_1 - a_1 & \text{if } a_1 = a_2 - 1 \\ m_1 + a_1 & \text{if } a_1 = a_2 + 1 \end{cases} \tag{56}$$

This makes the solution much more straightforward.

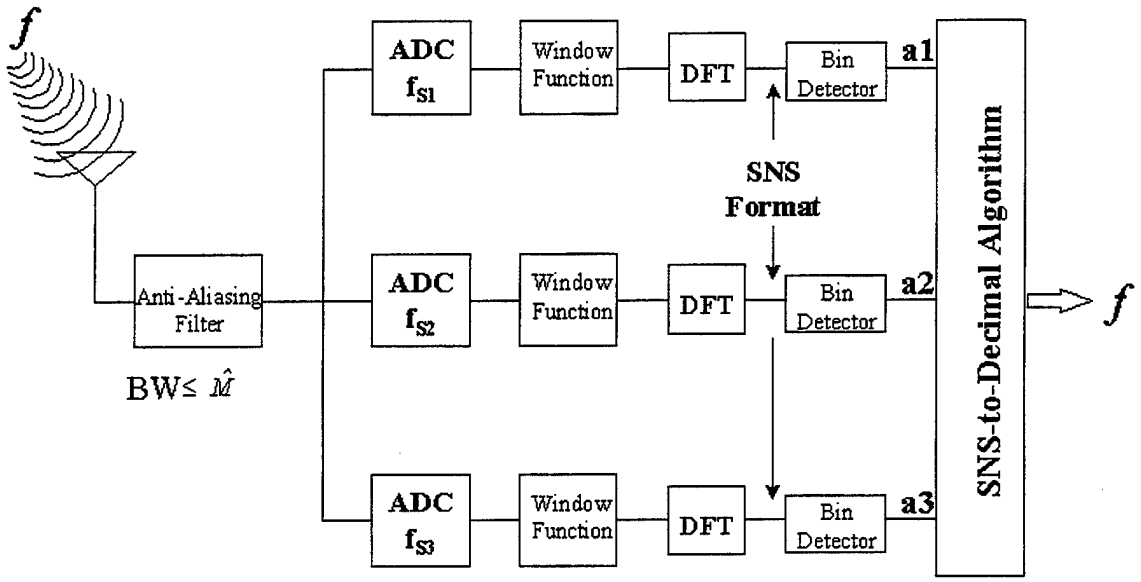

Figure 5.1: Block diagram of a three channel receiver architecture to determine a single frequency f

or

$$f \equiv \pm 252 \pm 70 \pm 120 \pmod{210}\ , \tag{58}$$

but $252 \pmod{210} \equiv 42 \pmod{210}$ so:

$$f \equiv \pm 42 \pm 70 \pm 120 \pmod{210}\ . \tag{59}$$

First,

$$f \equiv 42 + 70 + 120 \equiv 232 \equiv 22 (\mathrm{mod}\ 210)\ , \tag{60}$$

a value that can be discarded, because it and its negative are out of the dynamic range.

Second,

$$f \equiv 42 + 70 - 120 \equiv -8 (\mathrm{mod}\ 210)\ . \tag{61}$$

Although -8 is out of range, the negative, $f = 8$, is in the dynamic range, so that $f = 8$ is the correct frequency value.

VI. RESOLUTION OF TWO UNDERSAMPLED FREQUENCIES

A. DFT AMPLITUDE NORMALIZATION

Consider a unit amplitude signal containing a single integer frequency. After sampling and forming an N point DFT $X(k)$, the k^{th} bin corresponding to the digital frequency of the signal will have an amplitude $A(k)$ given by:

$$A(k) = \begin{cases} N & \text{if } k = 0, \text{ or } N_{\text{even}}/2 \\ N/2 & \text{elsewhere} \end{cases} \tag{62}$$

Dividing $X(k)$ by $A(k)$ will produce a normalized spectrum.

Figure 6.1 shows two DFTs of an undersampled signal containing two frequency components with unknown amplitude and frequency. Figure 6.1a displays the frequency spectrum for $f_{s1} = 10$ while Figure 6.1b corresponds to $f_{s2} = 11$. The two frequencies are known to lie within the dynamic range of the SNS system which in this case corresponds to $f < 15$. It is difficult to determine which two SNS pairs are valid by looking at the spectra of Figure 6.1. That is, either the bin pairs $\begin{bmatrix}1\\2\end{bmatrix}, \begin{bmatrix}4\\3\end{bmatrix}$ are correct or $\begin{bmatrix}1\\3\end{bmatrix}, \begin{bmatrix}4\\2\end{bmatrix}$ are correct.

B. BENEFITS OF NORMALIZATION

The benefits of normalizing the DFT are shown in Figures 6.2a and 6.2b where each of the original spectra have been divided by $A_1(k)$ and $A_2(k)$ respectively. In this case $N_1 = 10$ and $N_2 = 11$. It is now easy to see which magnitudes "match-up" and that $\begin{bmatrix}1\\2\end{bmatrix}, \begin{bmatrix}4\\3\end{bmatrix}$ is the correct set. Using the special case of two SNS moduli presented in Chapter IV, $m_1 = 2p$ and $m_2 = 2p + 1$ where $p = 5$, it is determined that $\begin{bmatrix}1\\2\end{bmatrix}, \begin{bmatrix}4\\3\end{bmatrix}$ corresponds to f=9 and f=14 with amplitudes 0.7514 and 0.6515 respectively.

Theorem 6.1 *Let f_{s1} and f_{s2} be any two relatively prime sampling frequencies. Considering a signal containing two unknown integer frequencies with distinct amplitudes,*

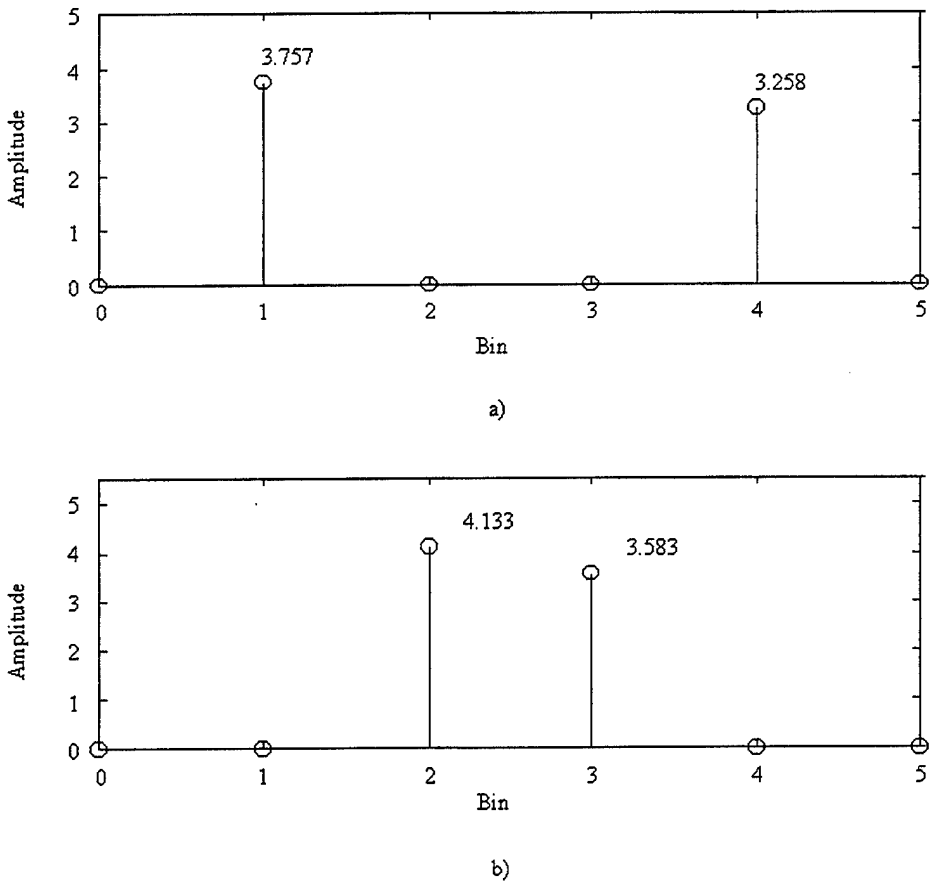

Figure 6.1: DFT for two unknown frequencies for a) $f_{s1} = 10$ and b) $f_{s2} = 11$.

the N-point normalized DFTs reveal two unique bin pairs which, in turn, reveal the two frequencies provided they are within the dynamic range of the SNS system.

C. SPECIAL CASE

The solution has a special case when the two frequencies alias to the same bin for one of the sampling frequencies. For example, incoming frequencies $f = 3$ and $f = 13$ would both alias into bin 3 for $f_{s1} = 10$ but into bins 3 and 2 for $f_{s2} = 11$. Normalization of the DFT will still produce accurate results as the magnitudes at bins 2 and 3 for $f_{s2} = 11$ will add up to the magnitude of bin 2 for $f_{s1} = 10$ and the

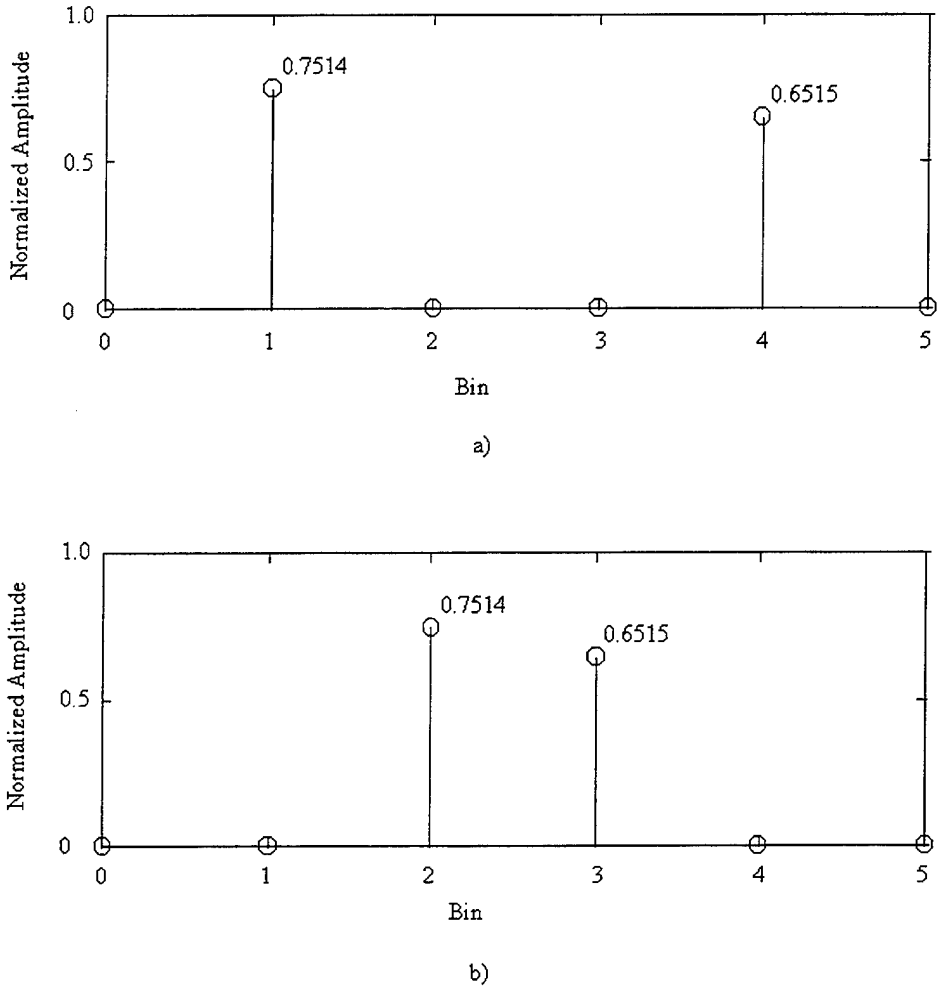

Figure 6.2: Normalized DFT for two unknown frequencies for a) $f_{s1} = 10$ and b) $f_{s2} = 11$.

bin pairs $\begin{bmatrix}3\\3\end{bmatrix}, \begin{bmatrix}3\\2\end{bmatrix}$ will yield the correct frequencies. When two frequencies are received with identical amplitudes, Theorem 6.1 does not apply.

Having shown that normalization allows us to "see" which bin pairs "match", normalization can also be used to measure how much energy went into each bin. If two frequencies land in the same bin, the normalized energy should essentially add together into that bin. This information along with bin location is used in the next chapter to solve for an entire spectrum of frequencies.

VII. INTRODUCTION TO RESOLVING MULTIPLE FREQUENCIES

A. SETTING UP THE SOLUTION

The normalization of the DFT amplitude introduced in the previous chapter leads to the consideration of a method to resolve any number of zero-phase frequencies which have no DFT leakage. By zero-phase frequencies with no leakage it is meant that the DFT values will be all real and that each resolves its entire energy into one DFT bin with no leakage.

Consider a bandlimited signal with frequency components that can range from 0 to 10 Hz. The amplitude and frequency of any component is unknown except that they are integer frequencies. Let $x_0, x_1, \cdots, x_{10}$ represent the amplitudes of each frequency component from f=0 Hz to f=10 Hz. Assume that the signal is sampled at f_{s1}=10 Hz and f_{s2}=11 Hz and that the DFT is applied and normalized. Two normalized spectra will be formed, each containing undersampling ambiguities for $f > 5$. Let the notation $b_{i,m}$ represent the value of the normalized DFT coefficient for bin i, $f_s = m$. From knowledge of aliasing it is clear that:

$$\begin{aligned}
b_{1,10} &= x_1 + x_9 \\
b_{2,10} &= x_2 + x_8 \\
b_{3,10} &= x_3 + x_7 \\
b_{4,10} &= x_4 + x_6 \\
b_{5,10} &= x_5 \\
b_{5,11} &= x_5 + x_6 \\
b_{4,11} &= x_4 + x_7 \\
b_{3,11} &= x_3 + x_8 \\
b_{2,11} &= x_2 + x_9 \\
b_{1,11} &= x_1 + x_{10} \\
b_{0,11} &= x_0
\end{aligned} \tag{63}$$

In other words, for $f_{s1} = 10$, $f = 1$ and $f = 9$ alias into bin 1, while $f = 2$ and $f = 8$ alias into bin 2, and so on. This forms a set of linear equations that can

be written as:

$$\begin{bmatrix} 0 & 1 & 0 & 0 & 0 & 0 & 0 & 0 & 0 & 1 & 0 \\ 0 & 0 & 1 & 0 & 0 & 0 & 0 & 0 & 1 & 0 & 0 \\ 0 & 0 & 0 & 1 & 0 & 0 & 0 & 1 & 0 & 0 & 0 \\ 0 & 0 & 0 & 0 & 1 & 0 & 1 & 0 & 0 & 0 & 0 \\ 0 & 0 & 0 & 0 & 0 & 1 & 0 & 0 & 0 & 0 & 0 \\ 0 & 0 & 0 & 0 & 0 & 1 & 1 & 0 & 0 & 0 & 0 \\ 0 & 0 & 0 & 0 & 1 & 0 & 0 & 1 & 0 & 0 & 0 \\ 0 & 0 & 0 & 1 & 0 & 0 & 0 & 0 & 1 & 0 & 0 \\ 0 & 0 & 1 & 0 & 0 & 0 & 0 & 0 & 0 & 1 & 0 \\ 0 & 1 & 0 & 0 & 0 & 0 & 0 & 0 & 0 & 0 & 1 \\ 1 & 0 & 0 & 0 & 0 & 0 & 0 & 0 & 0 & 0 & 0 \end{bmatrix} \begin{bmatrix} x_0 \\ x_1 \\ x_2 \\ x_3 \\ x_4 \\ x_5 \\ x_6 \\ x_7 \\ x_8 \\ x_9 \\ x_{10} \end{bmatrix} = \begin{bmatrix} b_{1,10} \\ b_{2,10} \\ b_{3,10} \\ b_{4,10} \\ b_{5,10} \\ b_{5,11} \\ b_{4,11} \\ b_{3,11} \\ b_{2,11} \\ b_{1,11} \\ b_{0,11} \end{bmatrix} \tag{64}$$

This is of the form $Ax = b$ where x represents the actual amplitudes of each frequency component and b represents the total amplitude that is aliased into each bin for the two sampling frequencies. From (63) it is easily seen that the values x_0 through x_{10} may be uniquely solved for. To begin with $x_0 = b_{0,11}$ and $x_5 = b_{5,10}$. Then the values x_0, x_4, x_7, etc., may be solved for successively. Thus, A is nonsingular and $x = A^{-1}b$:

$$\begin{bmatrix} x_0 \\ x_1 \\ x_2 \\ x_3 \\ x_4 \\ x_5 \\ x_6 \\ x_7 \\ x_8 \\ x_9 \\ x_{10} \end{bmatrix} = \begin{bmatrix} 0 & 0 & 0 & 0 & 0 & 0 & 0 & 0 & 0 & 0 & 1 \\ 1 & 1 & 1 & 1 & 1 & -1 & -1 & -1 & -1 & 0 & 0 \\ 0 & 1 & 1 & 1 & 1 & -1 & -1 & -1 & 0 & 0 & 0 \\ 0 & 0 & 1 & 1 & 1 & -1 & -1 & 0 & 0 & 0 & 0 \\ 0 & 0 & 0 & 1 & 1 & -1 & 0 & 0 & 0 & 0 & 0 \\ 0 & 0 & 0 & 0 & 1 & 0 & 0 & 0 & 0 & 0 & 0 \\ 0 & 0 & 0 & 0 & -1 & 1 & 0 & 0 & 0 & 0 & 0 \\ 0 & 0 & 0 & -1 & -1 & 1 & 1 & 0 & 0 & 0 & 0 \\ 0 & 0 & -1 & -1 & -1 & 1 & 1 & 1 & 0 & 0 & 0 \\ 0 & -1 & -1 & -1 & -1 & 1 & 1 & 1 & 1 & 0 & 0 \\ -1 & -1 & -1 & -1 & -1 & 1 & 1 & 1 & 1 & 1 & 0 \end{bmatrix} \begin{bmatrix} b_{1,10} \\ b_{2,10} \\ b_{3,10} \\ b_{4,10} \\ b_{5,10} \\ b_{5,11} \\ b_{4,11} \\ b_{3,11} \\ b_{2,11} \\ b_{1,11} \\ b_{0,11} \end{bmatrix} \tag{65}$$

From (65), it is now possible to reconstruct the original spectrum based upon the normalized bin values for the two undersampled spectra. Where before only frequencies from 0 to 5 Hz could be recovered, 65 allows integer frequencies from 0 to 10 Hz to be unambiguously recovered. It can be noted that the A matrix is 11×11 and that the additional equation for bin $b_{0,10}$ was not included. It turns out that including this bin does not add any additional information.

B. EXAMPLE

Suppose we have an incoming signal,

$$\begin{aligned} s(t) &= x_0 + x_1\cos(2\pi t) + x_2\cos(4\pi t) + x_3\cos(6\pi t) + x_4\cos(8\pi t) + \\ &\quad x_5\cos(10\pi t) + x_6\cos(12\pi t) + x_7\cos(14\pi t) + x_8\cos(16\pi t) + \\ &\quad x_9\cos(18\pi t) + x_{10}\cos(20\pi t) \end{aligned} \tag{66}$$

All x_n are unknown. The signal is sampled at $f_{s1} = 10$ Hz and $f_{s2} = 11$ Hz and the DFT is applied to both with N_1=10 and N_2=11 points respectively. This produces two spectra where any frequencies from 6 to 10 Hz are aliased into bins from 0 to 5 Hz. Both DFT's are normalized and the results for bins 0 through 5 are shown in Figure 7.1a for f_{s1}=10 and Figure 7.1b for f_{s2}=11.

From the values in each bin it is possible to form the b vector

$$b^T = [0.894\ 1.211\ 2.072\ 1.960\ 0.384\ 0.903\ 2.762\ 1.283\ 1.526\ 0.878\ 0.218] \tag{67}$$

and set up the equation $x = A^{-1}b$ which yields:

$$x^T = [0.218\ 0.047\ 0.679\ 0.751\ 1.441\ 0.384\ 0.519\ 1.321\ 0.532\ 0.847\ 0.831] \tag{68}$$

The solution (68) can be compared with the actual values for the x_n which is done in Figure 7.2.

Figure 7.2a shows the normalized DFT spectrum that results from sampling the same signal at 20 Hz. Figure 7.2b plots the solution (68). The solution is exact.

The solution method presented so far does little good if only signals with zero-phase can be resolved. In the next chapter, it is investigated how the imaginary components of a signal alias into bins and the results are used to generalize the solution for signals with random phase.

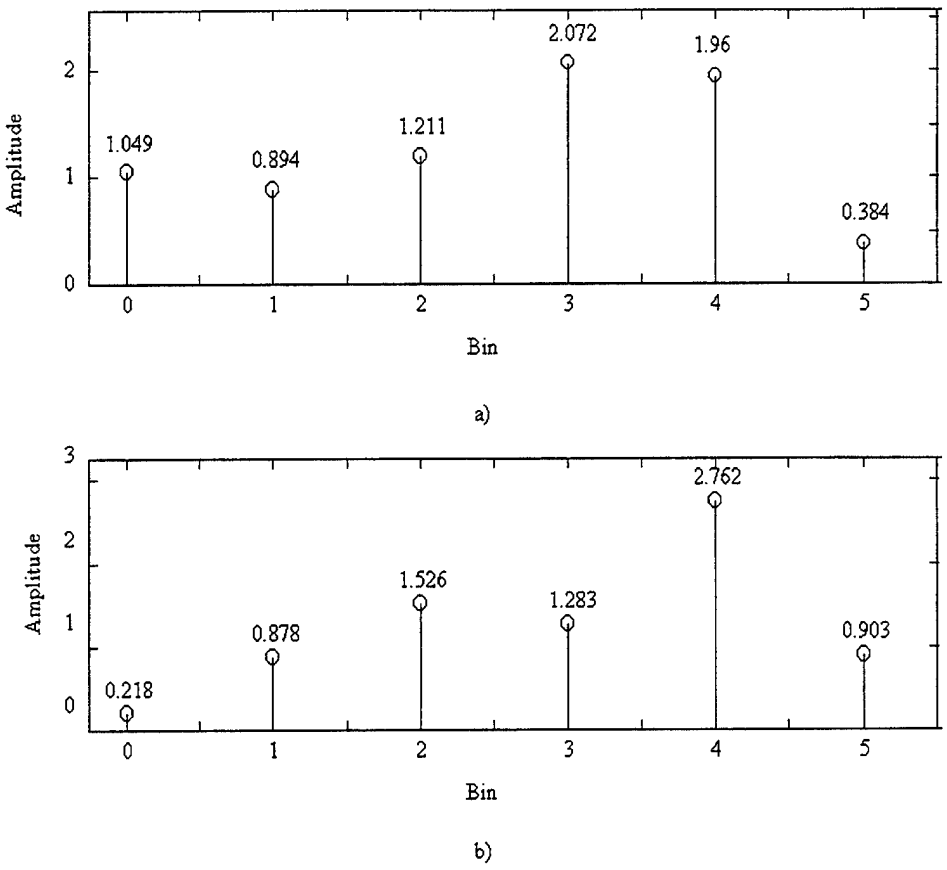

Figure 7.1: Normalized DFT for frequencies from 0 to 10 for a) $f_{s1} = 10$ and b) $f_{s2} = 11$.

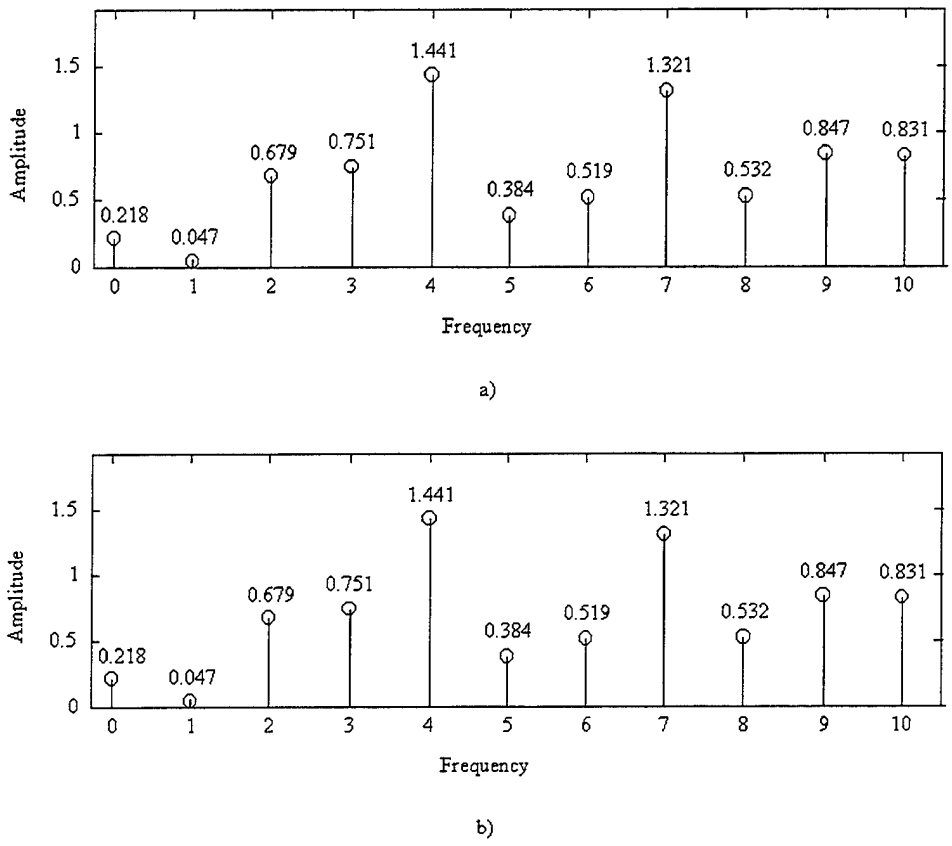

Figure 7.2: Frequency components and amplitudes: a) actual and b) calculated

VIII. RESOLVING MULTIPLE FREQUENCIES: FIRST ALGORITHM

A. CONSIDERING RANDOM PHASE SIGNALS

Thus far attention has been restricted to signals with zero phase. Consequently, the DFT yields an all real spectrum. When the frequency components have random phase, however, a modification to (65) must be introduced.

1. Illustration of Random Phase by Example

Consider a signal with integer frequency components from 0 to 10 Hz given by:

$$s(t) = x_0 + x_1\cos(2\pi t + \phi_1) + x_2\cos(4\pi t + \phi_2) + \cdots + x_{10}\cos(20\pi t + \phi_{10}) \quad (69)$$

where ϕ_n represents some random phase for each frequency component. If this signal was sampled at 20 Hz, DFT applied and normalized, bins 0 through 10 would have the values:

$$\begin{bmatrix} c_0 \\ c_1 \\ c_2 \\ \vdots \\ c_{10} \end{bmatrix} = \begin{bmatrix} x_0 \\ x_1\cos(\phi_1) + jx_1\sin(\phi_1) \\ x_2\cos(\phi_2) + jx_2\sin(\phi_2) \\ \vdots \\ x_{10}\cos(\phi_{10}) + jx_{10}\sin(\phi_{10}) \end{bmatrix} \quad (70)$$

where c_k represents the complex value of bin n and $c_k = a_k + jb_k$. If the same signal was sampled at 10 Hz, the DFT applied and normalized, the real part of each bin will be given by:

$$\begin{bmatrix} a_{1,10} \\ a_{2,10} \\ a_{3,10} \\ a_{4,10} \\ a_{5,10} \end{bmatrix} = \begin{bmatrix} x_1\cos(\phi_1) + x_9\cos(\phi_9) \\ x_2\cos(\phi_2) + x_8\cos(\phi_8) \\ x_3\cos(\phi_3) + x_7\cos(\phi_7) \\ x_4\cos(\phi_4) + x_6\cos(\phi_6) \\ x_5\cos(\phi_5) \end{bmatrix} \quad (71)$$

2. The Imaginary Component

Consider the imaginary component of each bin. If the DFT is treated as a unit circle as in Figure 3.1, then for f_s=10 Hz, all frequencies below 5 Hz lie in the top half of the unit circle and appear, without aliasing, in bins 0 through 5 of the DFT. All frequencies from 6 to 10 Hz, however, lie in the bottom half of the unit circle and alias back to the top half into bins 0 through 5 of the DFT. Since the real part of the DFT is an even function, the real components of the signals add together into bins 0 through 5. The imaginary component of the DFT is an odd function, however, and while the imaginary component of frequencies from 0 through 5 Hz add into bins 0 through 5, the imaginary components of frequencies from 6 through 10 Hz subtract. In other words:

$$\begin{bmatrix} b_{1,10} \\ b_{2,10} \\ b_{3,10} \\ b_{4,10} \\ b_{5,10} \end{bmatrix} = \begin{bmatrix} x_1 \sin(\phi_1) - x_9 \sin(\phi_9) \\ x_2 \sin(\phi_2) - x_8 \sin(\phi_8) \\ x_3 \sin(\phi_3) - x_7 \sin(\phi_7) \\ x_4 \sin(\phi_4) - x_6 \sin(\phi_6) \\ x_5 \sin(\phi_5) \end{bmatrix} \tag{72}$$

B. SOLVING FOR REAL AND IMAGINARY COMPONENTS

Based on how the imaginary components of the signals alias into the bins, it is again possible to form a set of linear equations.

$$\begin{bmatrix} b_{1,10} \\ b_{2,10} \\ b_{3,10} \\ b_{4,10} \\ b_{5,10} \\ b_{5,11} \\ b_{4,11} \\ b_{3,11} \\ b_{2,11} \\ b_{1,11} \\ b_{0,11} \end{bmatrix} = Imag \left(\begin{bmatrix} Z_1 - Z_9 \\ Z_2 - Z_8 \\ Z_3 - Z_7 \\ Z_4 - Z_6 \\ Z_5 \\ Z_5 - Z_6 \\ Z_4 - Z_7 \\ Z_3 - Z_8 \\ Z_2 - Z_9 \\ Z_1 - Z_{10} \\ Z_0 \end{bmatrix} \right) \tag{73}$$

or

$$\begin{bmatrix} 0 & 1 & 0 & 0 & 0 & 0 & 0 & 0 & 0 & -1 & 0 \\ 0 & 0 & 1 & 0 & 0 & 0 & 0 & 0 & -1 & 0 & 0 \\ 0 & 0 & 0 & 1 & 0 & 0 & 0 & -1 & 0 & 0 & 0 \\ 0 & 0 & 0 & 0 & 1 & 0 & -1 & 0 & 0 & 0 & 0 \\ 0 & 0 & 0 & 0 & 0 & 1 & 0 & 0 & 0 & 0 & 0 \\ 0 & 0 & 0 & 0 & 0 & 1 & -1 & 0 & 0 & 0 & 0 \\ 0 & 0 & 0 & 0 & 1 & 0 & 0 & -1 & 0 & 0 & 0 \\ 0 & 0 & 0 & 1 & 0 & 0 & 0 & 0 & -1 & 0 & 0 \\ 0 & 0 & 1 & 0 & 0 & 0 & 0 & 0 & 0 & -1 & 0 \\ 0 & 1 & 0 & 0 & 0 & 0 & 0 & 0 & 0 & 0 & -1 \\ 1 & 0 & 0 & 0 & 0 & 0 & 0 & 0 & 0 & 0 & 0 \end{bmatrix} \begin{bmatrix} Y_0 \\ Y_1 \\ Y_2 \\ Y_3 \\ Y_4 \\ Y_5 \\ Y_6 \\ Y_7 \\ Y_8 \\ Y_9 \\ Y_{10} \end{bmatrix} = \begin{bmatrix} b_{1,10} \\ b_{2,10} \\ b_{3,10} \\ b_{4,10} \\ b_{5,10} \\ b_{5,11} \\ b_{4,11} \\ b_{3,11} \\ b_{2,11} \\ b_{1,11} \\ b_{0,11} \end{bmatrix} \tag{74}$$

where $Z_n = x_n(\cos(\phi_n) + j\sin(\phi_n)) = X_n + jY_n$ and may be thought of as the normalized real and imaginary components of the signal for frequencies 0 through 10 Hz. The solution (74) may be written as $A_iY = b$. A_i has an inverse A_i^{-1} which can be seen in the same manner as A had an inverse in Chapter VII and (74) may be written as $Y = A_i^{-1}b$ or:

$$\begin{bmatrix} Y_0 \\ Y_1 \\ Y_2 \\ Y_3 \\ Y_4 \\ Y_5 \\ Y_6 \\ Y_7 \\ Y_8 \\ Y_9 \\ Y_{10} \end{bmatrix} = \begin{bmatrix} 0 & 0 & 0 & 0 & 0 & 0 & 0 & 0 & 0 & 0 & 1 \\ 1 & 1 & 1 & 1 & 1 & -1 & -1 & -1 & -1 & 0 & 0 \\ 0 & 1 & 1 & 1 & 1 & -1 & -1 & -1 & 0 & 0 & 0 \\ 0 & 0 & 1 & 1 & 1 & -1 & -1 & 0 & 0 & 0 & 0 \\ 0 & 0 & 0 & 1 & 1 & -1 & 0 & 0 & 0 & 0 & 0 \\ 0 & 0 & 0 & 0 & 1 & 0 & 0 & 0 & 0 & 0 & 0 \\ 0 & 0 & 0 & 0 & 1 & -1 & 0 & 0 & 0 & 0 & 0 \\ 0 & 0 & 0 & 1 & 1 & -1 & -1 & 0 & 0 & 0 & 0 \\ 0 & 0 & 1 & 1 & 1 & -1 & -1 & -1 & 0 & 0 & 0 \\ 0 & 1 & 1 & 1 & 1 & -1 & -1 & -1 & -1 & 0 & 0 \\ 1 & 1 & 1 & 1 & 1 & 1 & -1 & -1 & -1 & -1 & 0 \end{bmatrix} \begin{bmatrix} b_{1,10} \\ b_{2,10} \\ b_{3,10} \\ b_{4,10} \\ b_{5,10} \\ b_{5,11} \\ b_{4,11} \\ b_{3,11} \\ b_{2,11} \\ b_{1,11} \\ b_{0,11} \end{bmatrix} \tag{75}$$

which solves for the imaginary component while the real component is solved as in (65):

$$\begin{bmatrix} X_0 \\ X_1 \\ X_2 \\ X_3 \\ X_4 \\ X_5 \\ X_6 \\ X_7 \\ X_8 \\ X_9 \\ X_{10} \end{bmatrix} = \begin{bmatrix} 0 & 0 & 0 & 0 & 0 & 0 & 0 & 0 & 0 & 0 & 1 \\ 1 & 1 & 1 & 1 & 1 & -1 & -1 & -1 & -1 & 0 & 0 \\ 0 & 1 & 1 & 1 & 1 & -1 & -1 & -1 & 0 & 0 & 0 \\ 0 & 0 & 1 & 1 & 1 & -1 & -1 & 0 & 0 & 0 & 0 \\ 0 & 0 & 0 & 1 & 1 & -1 & 0 & 0 & 0 & 0 & 0 \\ 0 & 0 & 0 & 0 & 1 & 0 & 0 & 0 & 0 & 0 & 0 \\ 0 & 0 & 0 & 0 & -1 & 1 & 0 & 0 & 0 & 0 & 0 \\ 0 & 0 & 0 & -1 & -1 & 1 & 1 & 0 & 0 & 0 & 0 \\ 0 & 0 & -1 & -1 & -1 & 1 & 1 & 1 & 0 & 0 & 0 \\ 0 & -1 & -1 & -1 & -1 & 1 & 1 & 1 & 1 & 0 & 0 \\ -1 & -1 & -1 & -1 & -1 & 1 & 1 & 1 & 1 & 1 & 0 \end{bmatrix} \begin{bmatrix} a_{1,10} \\ a_{2,10} \\ a_{3,10} \\ a_{4,10} \\ a_{5,10} \\ a_{5,11} \\ a_{4,11} \\ a_{3,11} \\ a_{2,11} \\ a_{1,11} \\ a_{0,11} \end{bmatrix} \tag{76}$$

In summary, when the incoming signal has components with random phase, both the real and imaginary components may be solved separately by the equations above.

C. THE PIVOTAL FREQUENCY

An inspection of the specific case presented illustrates that the bin information at $f = 5$ Hz can be thought of as pivotal in that its accuracy affects the solution for the entire spectrum. Unfortunately, while the phase for the frequency component at $f = 5$ Hz (in this case) is random, the phase of Z_5 is not. In all cases for an N-point DFT, where N is even, the imaginary component of the $N/2$ bin will be zero. Thus, although the real part of the solution will be accurate, the imaginary component will not. In order to solve this problem with the DFT for the simple case presented ($f_{s1} = 10$ Hz and $f_{s2} = 11$ Hz), the signal is band-limited from 0 to 5 Hz, sample at 11 Hz, apply the DFT and normalize. The value of this DFT at bin 5 will be the correct value which can replace the values in (75) and (76) for $b_{5,10}$ and $a_{5,10}$.

D. EXAMPLE

Suppose there is an incoming signal,

$$s(t) = 0.218 + 0.047\cos(2\pi t + 5.1369) + 0.679\cos(4\pi t + 4.7491) +$$

$$0.751\cos(6\pi t + 2.9044) + 1.441\cos(8\pi t + 5.9776) +$$
$$0.384\cos(10\pi t + 3.9756) + 0.519\cos(12\pi t + 2.7604) +$$
$$1.321\cos(14\pi t + 5.1817) + 0.532\cos(16\pi t + 4.3290) +$$
$$0.847\cos(18\pi t + 4.4121) + 0.831\cos(20\pi t + 6.2024) \quad (77)$$

Assuming these amplitudes and phases are unknown, the signal is sampled at $f_{s1} = 10$ Hz and $f_{s2} = 11$ Hz, the DFT is applied and normalized. Figure 8.1 displays the real and imaginary components of the normalized DFT for $f_{s1} = 10$ Hz. Figure 8.2 displays the real and imaginary components of the normalized DFT for $f_{s2} = 11$ Hz.

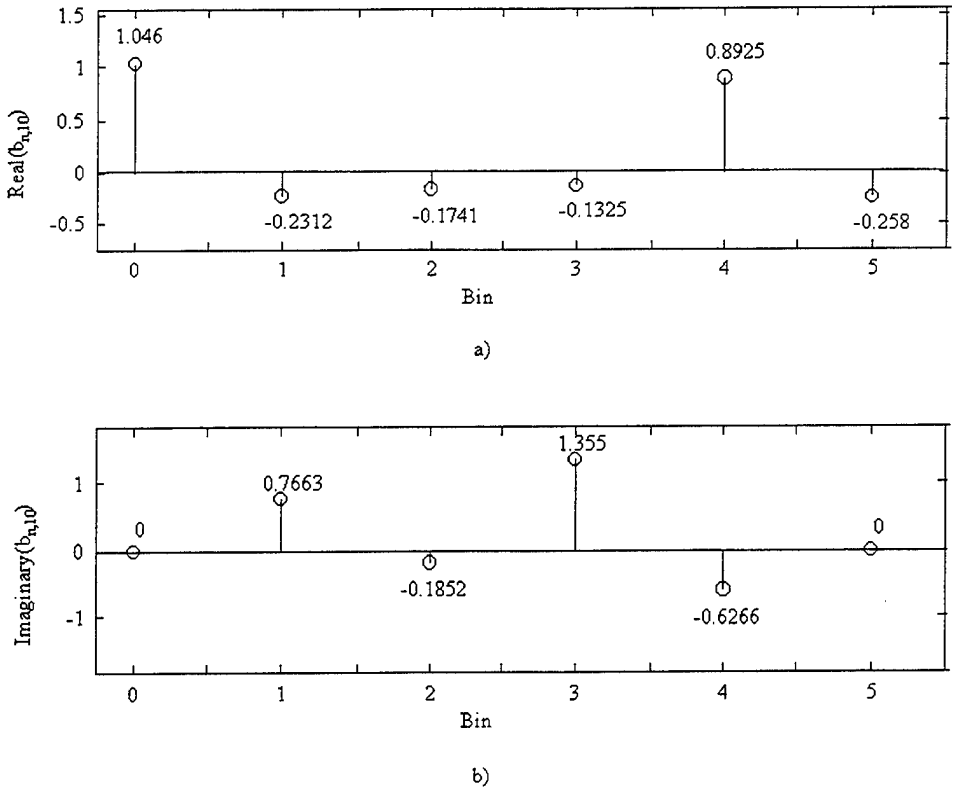

Figure 8.1: Normalized DFT components at $f_{s1} = 10$ Hz: a) real component and b) imaginary component.

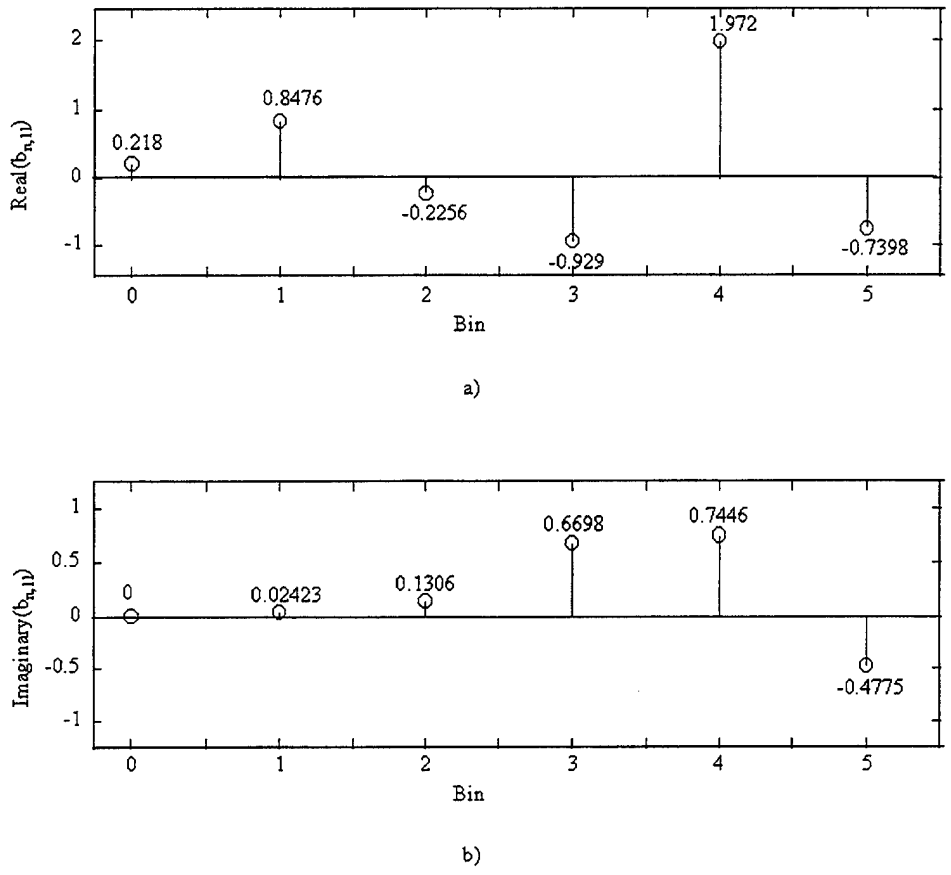

Figure 8.2: Normalized DFT components at f_{s2} = 11 Hz: a) real component and b) imaginary component.

Note from Figure 8.1b that $b_{5,10i} = 0$ which is the imaginary component of the fifth bin for f_{s1}=10. This is not the actual value and the actual value must be obtained by bandlimiting the signal between 0 and 5 Hz, sampling again at 11 Hz, and applying/normalizing the DFT. This yields the correct value for $b_{5,10} = -0.2844$. Now we may form the two vectors:

$$a^T = [-0.2312 \quad -0.1741 \quad -0.1325 \quad -0.8925 \quad -0.2580 \quad -0.7398 \quad 1.9717$$
$$-0.9290 \quad -0.2256 \quad 0.8476 \quad 0.2180]$$

and

$$b^T = [0.7663 \quad -0.1852 \quad 1.3546 \quad -0.6266 \quad -0.2844 \quad -0.4775 \quad 0.7446$$
$$0.6698 \quad 0.1306 \quad 0.0242 \quad 0.0000] \tag{78}$$

Solving $X = A_r^{-1}a$ and $Y = A_i^{-1}b$ yields:

$$\begin{bmatrix} Z_0 \\ Z_1 \\ Z_2 \\ Z_3 \\ Z_4 \\ Z_5 \\ Z_6 \\ Z_7 \\ Z_8 \\ Z_9 \\ Z_{10} \end{bmatrix} = \begin{bmatrix} 0.2180 \\ 0.0194 - j0.0428 \\ 0.0249 - j0.6785 \\ -0.7300 + j0.1765 \\ 1.3742 - j0.4335 \\ -0.2580 - j0.2844 \\ -0.4817 + j0.1931 \\ 0.5975 - j1.1782 \\ -0.1990 - j0.4934 \\ -0.2505 - j0.8091 \\ 0.8283 - j0.0671 \end{bmatrix} \tag{79}$$

A simple check reveals that this is the correct result.

This simple example helps to illustrate the solution method. Systems have been simulated in which $f_{s1} = 1000$ and $f_{s2} = 1001$ and exact results are attained in every case. One of the drawbacks of the solution is the need to band-limit the signal and sample a third time at f_{s2} in order to recover the phase of the frequency component at $f_{s1}/2$. An alternative method might be to simply not transmit that frequency or to use notch filters to eliminate that frequency and the problem associated with it.

E. REDUCING THE COMPUTING COST

Concerning the computing cost of the algorithm, if two full matrix multiplications are used every time to solve for the spectrum, computing cost becomes a factor as each matrix multiplication requires $0(N^2)$ multiplications and additions. About half of each inverse matrix is zeros and the solution could be hard-wired more efficiently to reduce flop counts.

F. GENERALIZING THE SOLUTION

Having presented the solution method by example, it is necessary to generalize the result for any two sampling frequencies.

Theorem 8.1 *Given $f_{s1} = N_1$ where N_1 is an even number and $f_{s2} = N_2 = N_1 + 1$, it is possible to form two N_2 x N_2 nonsingular matrices A_r and A_i which solve the system of equations $A_r X = a$ and $A_i Y = b$ given by:*

$$\begin{bmatrix} 0 & 1 & 0 & 0 & \cdots & 0 & 0 & 0 & 0 & \cdots & 0 & 0 & 1 & 0 \\ 0 & 0 & 1 & 0 & \cdots & 0 & 0 & 0 & 0 & \cdots & 0 & 1 & 0 & 0 \\ 0 & 0 & 0 & 1 & \cdots & 0 & 0 & 0 & 0 & \cdots & 1 & 0 & 0 & 0 \\ 0 & 0 & 0 & 0 & \cdots & 0 & 0 & 0 & 0 & \cdots & 0 & 0 & 0 & 0 \\ \vdots & \vdots & \vdots & \vdots & & \vdots & \vdots & \vdots & \vdots & & \vdots & \vdots & \vdots & \vdots \\ 0 & 0 & 0 & 0 & \cdots & 1 & 0 & 1 & 0 & \cdots & 0 & 0 & 0 & 0 \\ 0 & 0 & 0 & 0 & \cdots & 0 & 1 & 0 & 0 & \cdots & 0 & 0 & 0 & 0 \\ 0 & 0 & 0 & 0 & \cdots & 0 & 1 & 1 & 0 & \cdots & 0 & 0 & 0 & 0 \\ 0 & 0 & 0 & 0 & \cdots & 1 & 0 & 0 & 1 & \cdots & 0 & 0 & 0 & 0 \\ \vdots & \vdots & \vdots & \vdots & & \vdots & \vdots & \vdots & \vdots & & \vdots & \vdots & \vdots & \vdots \\ 0 & 0 & 0 & 1 & \cdots & 0 & 0 & 0 & 0 & \cdots & 0 & 1 & 0 & 0 \\ 0 & 0 & 1 & 0 & \cdots & 0 & 0 & 0 & 0 & \cdots & 0 & 0 & 1 & 0 \\ 0 & 1 & 0 & 0 & \cdots & 0 & 0 & 0 & 0 & \cdots & 0 & 0 & 0 & 1 \\ 1 & 0 & 0 & 0 & \cdots & 0 & 0 & 0 & 0 & \cdots & 0 & 0 & 0 & 0 \end{bmatrix} \begin{bmatrix} X_0 \\ X_1 \\ X_2 \\ X_3 \\ \vdots \\ X_{N_1/2-1} \\ X_{N_1/2} \\ X_{N_1/2+1} \\ X_{N_1/2+2} \\ \vdots \\ X_{N_1-3} \\ X_{N_1-2} \\ X_{N_1-1} \\ X_{N_1} \end{bmatrix} = \begin{bmatrix} a_{1,N_1} \\ a_{2,N_1} \\ a_{3,N_1} \\ a_{4,N_1} \\ \vdots \\ a_{N_1/2-1,N_1} \\ a_{N_1/2,N_1} \\ a_{N_1/2,N_2} \\ a_{N_1/2-1,N_2} \\ \vdots \\ a_{3,N_2} \\ a_{2,N_2} \\ a_{1,N_2} \\ a_{0,N_2} \end{bmatrix} \tag{80}$$

$$\begin{bmatrix} 0 & 1 & 0 & 0 & \cdots & 0 & 0 & 0 & 0 & \cdots & 0 & 0 & -1 & 0 \\ 0 & 0 & 1 & 0 & \cdots & 0 & 0 & 0 & 0 & \cdots & 0 & -1 & 0 & 0 \\ 0 & 0 & 0 & 1 & \cdots & 0 & 0 & 0 & 0 & \cdots & -1 & 0 & 0 & 0 \\ 0 & 0 & 0 & 0 & \cdots & 0 & 0 & 0 & 0 & \cdots & 0 & 0 & 0 & 0 \\ \vdots & \vdots & \vdots & \vdots & & \vdots & \vdots & \vdots & \vdots & & \vdots & \vdots & \vdots & \vdots \\ 0 & 0 & 0 & 0 & \cdots & 1 & 0 & -1 & 0 & \cdots & 0 & 0 & 0 & 0 \\ 0 & 0 & 0 & 0 & \cdots & 0 & 1 & 0 & 0 & \cdots & 0 & 0 & 0 & 0 \\ 0 & 0 & 0 & 0 & \cdots & 0 & 1 & -1 & 0 & \cdots & 0 & 0 & 0 & 0 \\ 0 & 0 & 0 & 0 & \cdots & 1 & 0 & 0 & -1 & \cdots & 0 & 0 & 0 & 0 \\ \vdots & \vdots & \vdots & \vdots & & \vdots & \vdots & \vdots & \vdots & & \vdots & \vdots & \vdots & \vdots \\ 0 & 0 & 0 & 1 & \cdots & 0 & 0 & 0 & 0 & \cdots & 0 & -1 & 0 & 0 \\ 0 & 0 & 1 & 0 & \cdots & 0 & 0 & 0 & 0 & \cdots & 0 & 0 & -1 & 0 \\ 0 & 1 & 0 & 0 & \cdots & 0 & 0 & 0 & 0 & \cdots & 0 & 0 & 0 & -1 \\ 1 & 0 & 0 & 0 & \cdots & 0 & 0 & 0 & 0 & \cdots & 0 & 0 & 0 & 0 \end{bmatrix} \begin{bmatrix} Y_0 \\ Y_1 \\ Y_2 \\ Y_3 \\ \vdots \\ Y_{N_1/2-1} \\ Y_{N_1/2} \\ Y_{N_1/2+1} \\ Y_{N_1/2+2} \\ \vdots \\ Y_{N_1-3} \\ Y_{N_1-2} \\ Y_{N_1-1} \\ Y_{N_1} \end{bmatrix} = \begin{bmatrix} b_{1,N_1} \\ b_{2,N_1} \\ b_{3,N_1} \\ b_{4,N_1} \\ \vdots \\ b_{N_1/2-1,N_1} \\ b_{N_1/2,N_1} \\ b_{N_1/2,N_2} \\ b_{N_1/2-1,N_2} \\ \vdots \\ b_{3,N_2} \\ b_{2,N_2} \\ b_{1,N_2} \\ b_{0,N_2} \end{bmatrix} \tag{81}$$

The inverses of A_r and A_i exist and the linear system may be solved $X = A_r^{-1}a$ and $Y = A_i^{-1}b$ given by:

$$\begin{bmatrix} X_0 \\ X_1 \\ X_2 \\ X_3 \\ \vdots \\ X_{N_1/2-1} \\ X_{N_1/2} \\ X_{N_1/2+1} \\ X_{N_1/2+2} \\ \vdots \\ X_{N_1-3} \\ X_{N_1-2} \\ X_{N_1-1} \\ X_{N_1} \end{bmatrix} = \begin{bmatrix} 0 & 0 & 0 & 0 & \cdots & 0 & 0 & 0 & 0 & \cdots & 0 & 0 & 0 & 1 \\ 1 & 1 & 1 & 1 & \cdots & 1 & 1 & -1 & -1 & \cdots & -1 & -1 & 0 & 0 \\ 0 & 1 & 1 & 1 & \cdots & 1 & 1 & -1 & -1 & \cdots & -1 & 0 & 0 & 0 \\ 0 & 0 & 1 & 1 & \cdots & 1 & 1 & -1 & -1 & \cdots & 0 & 0 & 0 & 0 \\ \vdots & \vdots & \vdots & \vdots & \vdots & \vdots & \vdots & \vdots & \vdots & \vdots & \vdots & \vdots & \vdots & \vdots \\ 0 & 0 & 0 & 0 & \cdots & 1 & 1 & -1 & 0 & \cdots & 0 & 0 & 0 & 0 \\ 0 & 0 & 0 & 0 & \cdots & 0 & 1 & 0 & 0 & \cdots & 0 & 0 & 0 & 0 \\ 0 & 0 & 0 & 0 & \cdots & 0 & -1 & 1 & 0 & \cdots & 0 & 0 & 0 & 0 \\ 0 & 0 & 0 & 0 & \cdots & -1 & -1 & 1 & 1 & \cdots & 0 & 0 & 0 & 0 \\ \vdots & \vdots & \vdots & \vdots & \vdots & \vdots & \vdots & \vdots & \vdots & \vdots & \vdots & \vdots & \vdots & \vdots \\ 0 & 0 & 0 & -1 & \cdots & -1 & -1 & 1 & 1 & \cdots & 0 & 0 & 0 & 0 \\ 0 & 0 & -1 & -1 & \cdots & -1 & -1 & 1 & 1 & \cdots & 1 & 0 & 0 & 0 \\ 0 & -1 & -1 & -1 & \cdots & -1 & -1 & 1 & 1 & \cdots & 1 & 1 & 0 & 0 \\ -1 & -1 & -1 & -1 & \cdots & -1 & -1 & 1 & 1 & \cdots & 1 & 1 & 1 & 0 \end{bmatrix} \begin{bmatrix} a_{1,N_1} \\ a_{2,N_1} \\ a_{3,N_1} \\ a_{4,N_1} \\ \vdots \\ a_{N_1/2-1,N_1} \\ a_{N_1/2,N_1} \\ a_{N_1/2,N_2} \\ a_{N_1/2-1,N_2} \\ \vdots \\ a_{3,N_2} \\ a_{2,N_2} \\ a_{1,N_2} \\ a_{0,N_2} \end{bmatrix} \tag{82}$$

$$\begin{bmatrix} Y_0 \\ Y_1 \\ Y_2 \\ Y_3 \\ \vdots \\ Y_{N_1/2-1} \\ Y_{N_1/2} \\ Y_{N_1/2+1} \\ Y_{N_1/2+2} \\ \vdots \\ Y_{N_1-3} \\ Y_{N_1-2} \\ Y_{N_1-1} \\ Y_{N_1} \end{bmatrix} = \begin{bmatrix} 0 & 0 & 0 & 0 & \cdots & 0 & 0 & 0 & 0 & \cdots & 0 & 0 & 0 & 1 \\ 1 & 1 & 1 & 1 & \cdots & 1 & 1 & -1 & -1 & \cdots & -1 & -1 & 0 & 0 \\ 0 & 1 & 1 & 1 & \cdots & 1 & 1 & -1 & -1 & \cdots & -1 & 0 & 0 & 0 \\ 0 & 0 & 1 & 1 & \cdots & 1 & 1 & -1 & -1 & \cdots & 0 & 0 & 0 & 0 \\ \vdots & \vdots & \vdots & \vdots & \vdots & \vdots & \vdots & \vdots & \vdots & \vdots & \vdots & \vdots & \vdots & \vdots \\ 0 & 0 & 0 & 0 & \cdots & 1 & 1 & -1 & 0 & \cdots & 0 & 0 & 0 & 0 \\ 0 & 0 & 0 & 0 & \cdots & 0 & 1 & 0 & 0 & \cdots & 0 & 0 & 0 & 0 \\ 0 & 0 & 0 & 0 & \cdots & 0 & 1 & -1 & 0 & \cdots & 0 & 0 & 0 & 0 \\ 0 & 0 & 0 & 0 & \cdots & 1 & 1 & -1 & -1 & \cdots & 0 & 0 & 0 & 0 \\ \vdots & \vdots & \vdots & \vdots & \vdots & \vdots & \vdots & \vdots & \vdots & \vdots & \vdots & \vdots & \vdots & \vdots \\ 0 & 0 & 0 & 1 & \cdots & 1 & 1 & -1 & -1 & \cdots & 0 & 0 & 0 & 0 \\ 0 & 0 & 1 & 1 & \cdots & 1 & 1 & -1 & -1 & \cdots & -1 & 0 & 0 & 0 \\ 0 & 1 & 1 & 1 & \cdots & 1 & 1 & -1 & -1 & \cdots & -1 & -1 & 0 & 0 \\ 1 & 1 & 1 & 1 & \cdots & 1 & 1 & -1 & -1 & \cdots & -1 & -1 & -1 & 0 \end{bmatrix} \begin{bmatrix} b_{1,N_1} \\ b_{2,N_1} \\ b_{3,N_1} \\ b_{4,N_1} \\ \vdots \\ b_{N_1/2-1,N_1} \\ b_{N_1/2,N_1} \\ b_{N_1/2,N_2} \\ b_{N_1/2-1,N_2} \\ \vdots \\ b_{3,N_2} \\ b_{2,N_2} \\ b_{1,N_2} \\ b_{0,N_2} \end{bmatrix} \tag{83}$$

All methods for solving undersampled signals so far have required at least two sampling frequencies. The additional complexity is a trade-off for the additional information gained. In the next chapter, however, a second algorithm is introduced which requires only one sampling frequency and simplifies the overall solution considerably.

IX. RESOLVING MULTIPLE FREQUENCIES: SECOND ALGORITHM

A. BACKGROUND

So far the solution method has required that an undersampled signal be sampled more than once with a different sampling frequency each time. It is, however, possible to undersample a signal more than once with a single sampling frequency yet still recover the original spectrum. In fact, the groundwork for such a system has already been laid in Chapter VIII. Recalling the discussion in Chapter VIII, Section C, the problems encountered with the pivotal frequency required that the signal be band-limited between 0 and $\frac{f_{s1}}{2}$ to recover the actual value of bin $c_{\frac{f_{s1}}{2},f_{s1}}$. It appeared to be a waste of time but a necessary evil to recover the correct bin information for this pivotal bin. Options discussed to remove this apparent constraint were to not transmit the frequency or use a notch filter to eliminate it before processing.

B. USING THE BANDLIMITED SPECTRUM

Consider a signal $s(t)$ which contains frequency components from 0 to f Hz of unknown magnitude and phase. Previously, the solution would have required that $s(t)$ be sampled at both $f_{s1} = f$ Hz and $f_{s2} = f+1$ Hz in order to recover the original spectrum. As discussed, the solution would also require that $s(t)$ be additionally bandlimited between 0 and $f/2$ Hz in order to recover the correct value for $c_{\frac{f_{s1}}{2},f_{s1}}$. Discarding all information gained from the band-limited spectrum, (82) and (83) would then be used to solve for the original spectrum. In fact, the solution method wastes time because the band-limited spectrum has no aliased components and the bin values correspond to the actual values for $Z_0, Z_1, ..., Z_{\frac{f}{2}}$.

1. Recovering the First Half of the Spectrum

Consider a signal, $s(t)$ containing frequency components from 0 to 10 Hz. If the signal is first bandlimited between 0 and 5 Hz and then sampled at 11 Hz, the actual frequency coefficients are given by:

$$\begin{bmatrix} Z_0 \\ Z_1 \\ Z_2 \\ Z_3 \\ Z_4 \\ Z_5 \end{bmatrix} = \begin{bmatrix} c_{0,11_L} \\ c_{1,11_L} \\ c_{2,11_L} \\ c_{3,11_L} \\ c_{4,11_L} \\ c_{5,11_L} \end{bmatrix} \tag{84}$$

where $Z_n = X_n + jY_n$ represents the actual real and imaginary component at the frequency of n Hz and $c_{n,f_{sL}} = a_{n,f_{sL}} + jb_{n,f_{sL}}$ corresponds to the value of the n_{th} bin at a sampling frequency of f_s. The additional L subscript denotes that this is the band-limited version of the signal.

2. Recovering the Other Half of the Spectrum

Suppose that on another channel the signal $s(t)$ is not band-limited. If $s(t)$ is sampled at 11 Hz and the DFT is applied and normalized the real components will go into bins as:

$$\begin{bmatrix} a_{0,11} \\ a_{1,11} \\ a_{2,11} \\ a_{3,11} \\ a_{4,11} \\ a_{5,11} \end{bmatrix} = \begin{bmatrix} X_0 \\ X_1 + X_{10} \\ X_2 + X_9 \\ X_3 + X_8 \\ X_4 + X_7 \\ X_5 + X_6 \end{bmatrix} \tag{85}$$

while the imaginary components go into bins as:

$$\begin{bmatrix} b_{0,11} \\ b_{1,11} \\ b_{2,11} \\ b_{3,11} \\ b_{4,11} \\ b_{5,11} \end{bmatrix} = \begin{bmatrix} 0 \\ Y_1 - Y_{10} \\ Y_2 - Y_9 \\ Y_3 - Y_8 \\ Y_4 - Y_7 \\ Y_5 - Y_6 \end{bmatrix} \tag{86}$$

Substituting the values for the Z_n's from (84), (85) and (86) may be re-written as:

$$\begin{bmatrix} X_{10} \\ X_9 \\ X_8 \\ X_7 \\ X_6 \end{bmatrix} = \begin{bmatrix} a_{1,11} - a_{1,11_L} \\ a_{2,11} - a_{2,11_L} \\ a_{3,11} - a_{3,11_L} \\ a_{4,11} - a_{4,11_L} \\ a_{5,11} - a_{5,11_L} \end{bmatrix} \tag{87}$$

and

$$\begin{bmatrix} Y_{10} \\ Y_9 \\ Y_8 \\ Y_7 \\ Y_6 \end{bmatrix} = - \begin{bmatrix} b_{1,11} - b_{1,11_L} \\ b_{2,11} - b_{2,11_L} \\ b_{3,11} - b_{3,11_L} \\ b_{4,11} - b_{4,11_L} \\ b_{5,11} - b_{5,11_L} \end{bmatrix} \tag{88}$$

Combining (84), (87), and (88) yields:

$$\begin{bmatrix} Z_0 \\ Z_1 \\ Z_2 \\ Z_3 \\ Z_4 \\ Z_5 \\ Z_6 \\ Z_7 \\ Z_8 \\ Z_9 \\ Z_{10} \end{bmatrix} = \begin{bmatrix} c_{0,11_L} \\ c_{1,11_L} \\ c_{2,11_L} \\ c_{3,11_L} \\ c_{4,11_L} \\ c_{5,11_L} \\ \text{conj} \begin{pmatrix} c_{5,11} - c_{5,11_L} \\ c_{4,11} - c_{4,11_L} \\ c_{3,11} - c_{3,11_L} \\ c_{2,11} - c_{2,11_L} \\ c_{1,11} - c_{1,11_L} \end{pmatrix} \end{bmatrix} \tag{89}$$

As can be seen, the solution is much simpler requiring only one sampling frequency and far fewer computations.

C. GENERAL SOLUTION

Figure 9.1 displays a possible architecture to resolve an undersampled signal using the method described. The incoming signal is split into two branches. The top branch is the band-limited branch and solves for the first half of the spectrum. This information is then combined with the information from the bottom branch to recover the undersampled spectrum.

The solution (89) can be generalized:

Theorem 9.1 *Let the sampling frequency of a system be f_s where f_s is any odd number. A spectrum containing frequencies between 0 and $f_s - 1$ Hz may be unambiguously recovered provided that a copy of the signal is also band-limited to recover the spectrum between 0 and $\frac{f_s-1}{2}$. This information is then used to recover the other half of the spectrum as in:*

$$\begin{bmatrix} Z_0 \\ Z_1 \\ Z_2 \\ \vdots \\ Z_{\frac{f_s-1}{2}-2} \\ Z_{\frac{f_s-1}{2}-1} \\ Z_{\frac{f_s-1}{2}} \\ Z_{\frac{f_s-1}{2}+1} \\ Z_{\frac{f_s-1}{2}+2} \\ Z_{\frac{f_s-1}{2}+3} \\ \vdots \\ Z_{f_s-3} \\ Z_{f_s-2} \\ Z_{f_s-1} \end{bmatrix} = \begin{bmatrix} c_{0,f_{sL}} \\ c_{1,f_{sL}} \\ c_{2,f_{sL}} \\ \vdots \\ c_{\frac{f_s-1}{2}-2,f_{sL}} \\ c_{\frac{f_s-1}{2}-1,f_{sL}} \\ c_{\frac{f_s-1}{2},f_{sL}} \\ conj \begin{pmatrix} c_{\frac{f_s-1}{2},f_s} - c_{\frac{f_s-1}{2},f_{sL}} \\ c_{\frac{f_s-1}{2}-1,f_s} - c_{\frac{f_s-1}{2}-1,f_{sL}} \\ c_{\frac{f_s-1}{2}-2,f_s} - c_{\frac{f_s-1}{2}-2,f_{sL}} \\ \vdots \\ c_{3,f_s} - c_{3,f_{sL}} \\ c_{2,f_s} - c_{2,f_{sL}} \\ c_{1,f_s} - c_{1,f_{sL}} \end{pmatrix} \end{bmatrix} \tag{90}$$

where $Z_n = X_n + jY_n$ and $c_{n,m} = a_{n,m} + jb_{n,m}$.

It would be nice to know that (9.1) puts the Nyquist criterion to rest once and for all but a fair treatment requires that the problems with the methods described be explored. The next chapter discusses the current limitations of the algorithms as well as potentially resolving the same limitations.

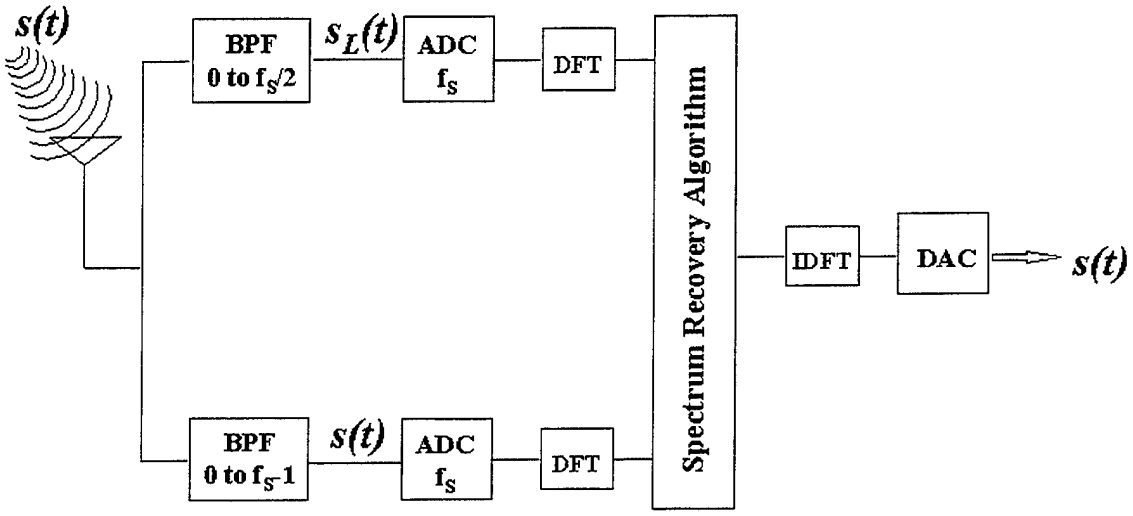

Figure 9.1: Channel architecture to resolve an undersampled signal utilizing a single sampling frequency

X. PROBLEMS WITH THE SOLUTION

A. SIGNALS THAT CAUSE DFT LEAKAGE

So far only frequencies which directly resolve into single bins without leakage have been considered. There is a problem with the solution when the incoming frequency components lie in between DFT bins and leakage occurs. When the DFT is applied to a sequence with frequencies that correspond directly to DFT bins, the result is that the components resolve all of their energy into the bins of the DFT. This is not so with frequencies that "straddle" bins.

B. DFT LEAKAGE EXAMPLES

Consider a signal containing just one frequency at 2.3153 Hz, given by:

$$s(t) = \cos(2\pi(2.3153)t) \tag{91}$$

Note that the signal has zero phase. Unfortunately, instead of resolving into just bin 2 when sampled, the side-lobes of the DFT distribute a portion of the energy into many bins.

1. Algorithm of Theorem 8.1

Using the algorithm of Theorem 8.1, the signal is sampled at both 10 and 11 Hz, the DFT and normalized with results shown in Figure 10.1. Displayed are the real and imaginary components of the DFT. These DFT results along with (82) and (83) yield the spectrum shown in Figure 10.2a for the real part and Figure 10.2b for the imaginary part. The result is clearly inaccurate.

2. Algorithm of Theorem 9.1

The algorithm of Theorem 9.1 is not nearly as inaccurate for a single frequency. Figure 10.1c and Figure 10.1d correspond to both the band-limited and normal spectrums which would be used to solve for the original spectrum. The answer would be

exact. The algorithm's strength lies in the fact that half of the solution is determined exactly in the top branch of Figure 9.1. The solution is not totally immune to the effects of DFT leakage however. As an example, assume a signal $s(t)$ has frequency components in $\frac{1}{2}$ Hz increments from 0 to 10 Hz (0, .5, 1, 1.5, ..., 9.5, 10). The sampling frequency is 11 Hz. Figures 10.3a and 10.3b display the real and imaginary spectra of the band-limited version of the signal after sampling and DFT normalization while figures 10.3c and 10.3d display the non-bandlimited spectra after sampling and DFT normalization. Utilizing (90), the original spectrum is calculated and plotted in Figures 10.4a and 10.4b while Figures 10.4c and 10.4d show the actual values. The solution is inaccurate.

C. LEAKAGE AND SOLUTION INSTABILITY

It is not too difficult to discern why the solution methods are unstable. One might think that perhaps the leakage from all the other frequencies would somehow combine in such a way that the relative magnitudes of the resulting spectrum would remain intact. Unfortunately, the symmetrical number system and the linear solutions presented both depend on nearly all energy being within the bin that it is expected to be in. As an example consider if an incoming frequency at 2 Hz correctly processes totally into bin 2 at 10 Hz but somehow processes into bin 3 at 11 Hz. Whereas the correct solution is for all energy to be at f = 2 Hz in the final spectrum, this small bin error will result in calculating that all energy belongs to f = 8 Hz.

D. SOLVING THE PROBLEM?

What is needed ideally is some sort of transformation that places all energy in the expected bins without leakage. For instance, for $f_{s1} = 10$ it is desired that $f \geq 9.5$ and $0 \leq f \leq 0.5$ to resolve into bin 0, $0.5 \leq f \leq 1.5$ to resolve into bin 1, $\cdots$, and $8.5 \leq f \leq 9.5$ to resolve totally into bin 9. Clearly no such transformation

exists which will resolve a spectrum exactly without leakage. There is one direction, however, that may contain some promise.

Consider again our signal, $s(t)$, with a single frequency at 2.3153 Hz. Sample again at 10 and 11 Hz but this time sample for 100 seconds instead of just 1 second. Applying the DFT and normalizing, the DFT now has a bin resolution of 0.01 seconds instead of just 1 second. This means that any incoming frequency at any integer multiple of 0.01 Hz will resolve exactly into a single bin while all others will cause leakage. The results of the DFTs are shown in Figure 10.5. Figure 10.5 shows the effect of increasing the bin resolution which has the effect of containing the energy within the area of interest. The sidelobes decay well before they "leak" much into any of the other bin boundaries. Still, while the energy is now contained in the region of interest, there needs to be a method to recover the overall real and complex portions of the signal that belong to each integer bin. In the case studied, the goal is to find the energy that resolves into the five bins for $f_{s1} = 10$ Hz and $f_{s2} = 11$ Hz, respectively, and use the linear equations presented to solve for the spectrum with a bin resolution of 1 Hz.

For the algorithm of Theorem 9.1 the same benefits apply. In fact, increasing the bin resolution may hold even more promise. The algorithm holds up fairly well when only a little leakage occurs but falls apart when leakage increases.

It should be emphasized that 10 and 11 Hz have been used as sampling frequencies throughout for simplicity of presentation. Preliminary study has shown that a separation of 1 between the two sampling frequencies gives the best dynamic range with the lowest sampling frequencies. It can be shown easily, for instance, that the dynamic range of the algorithm of theorem 8.1 is still 0 to 10 Hz for sampling frequencies of 10 and 12 Hz.

Another aspect of theorem 8.1 is that, unlike the multiplicative nature of the dynamic range with the symmetrical number system, the dynamic range of the solution is additive. It depends upon the number of linearly independent equations that can be set up based upon the number of bins for each sampling frequency used. For this reason, this algorithm would be most cost-performance efficient using just two sampling frequencies as presented.

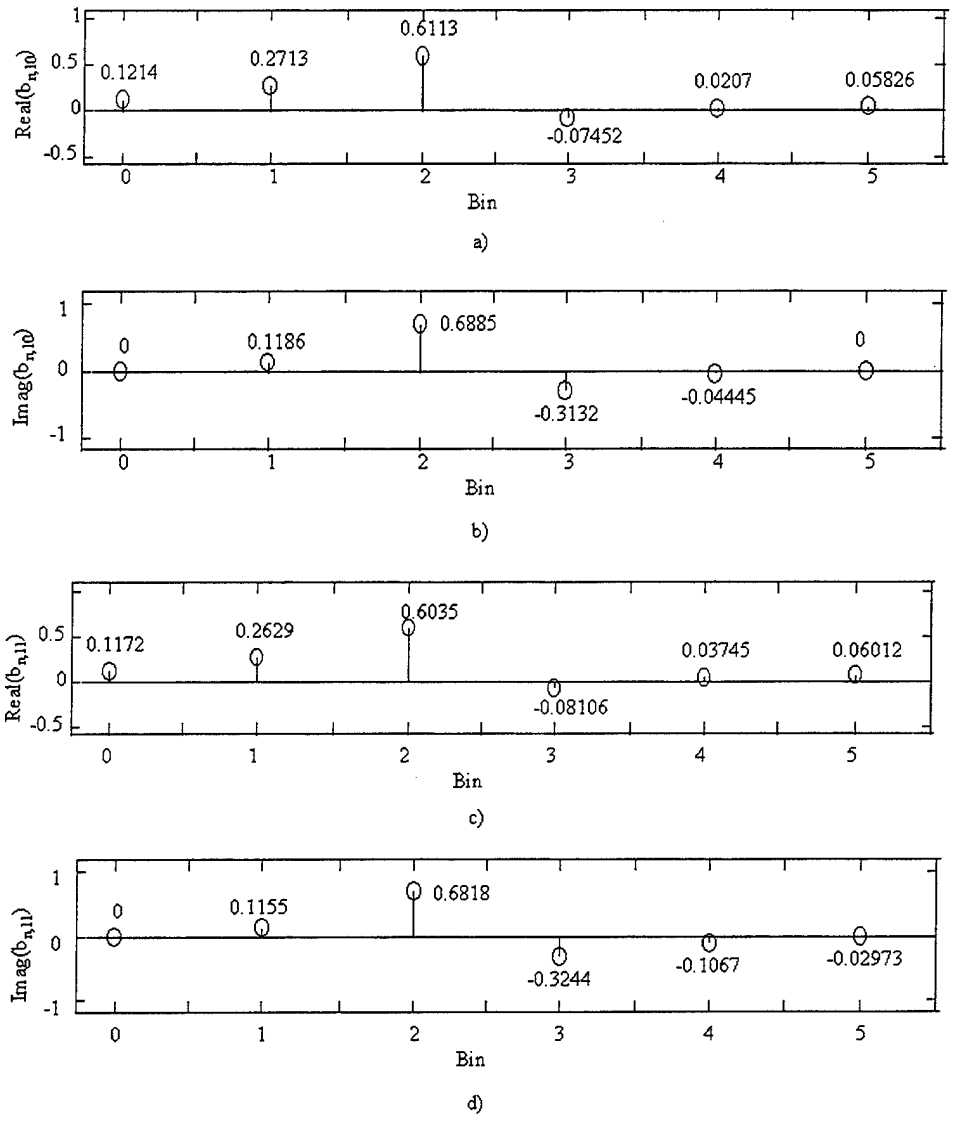

Figure 10.1: Normalized DFT of sinusoid at $f = 2.3153$ Hz: a) real component for $f_{s1} = 10$ Hz, b) imaginary component for $f_{s1} = 10$ Hz, c) real component for $f_{s2} = 11$ Hz, and d) imaginary component for $f_{s2} = 11$ Hz.

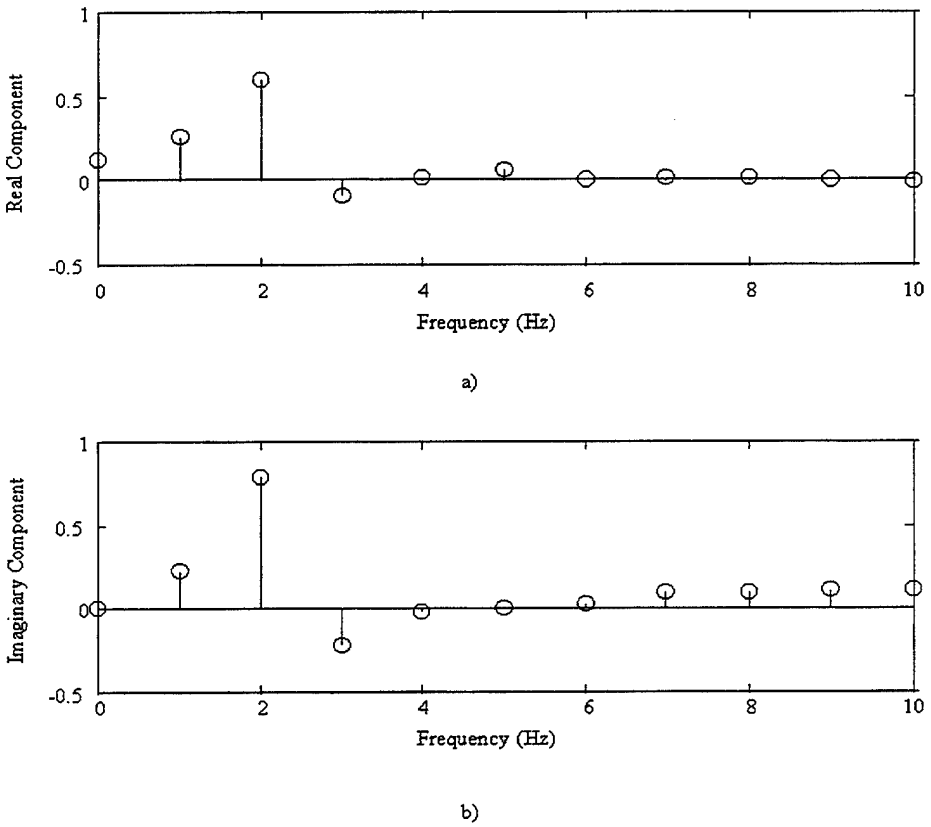

Figure 10.2: Spectrum calculated for single frequency at 2.3153 Hz: a) real component and b) imaginary component

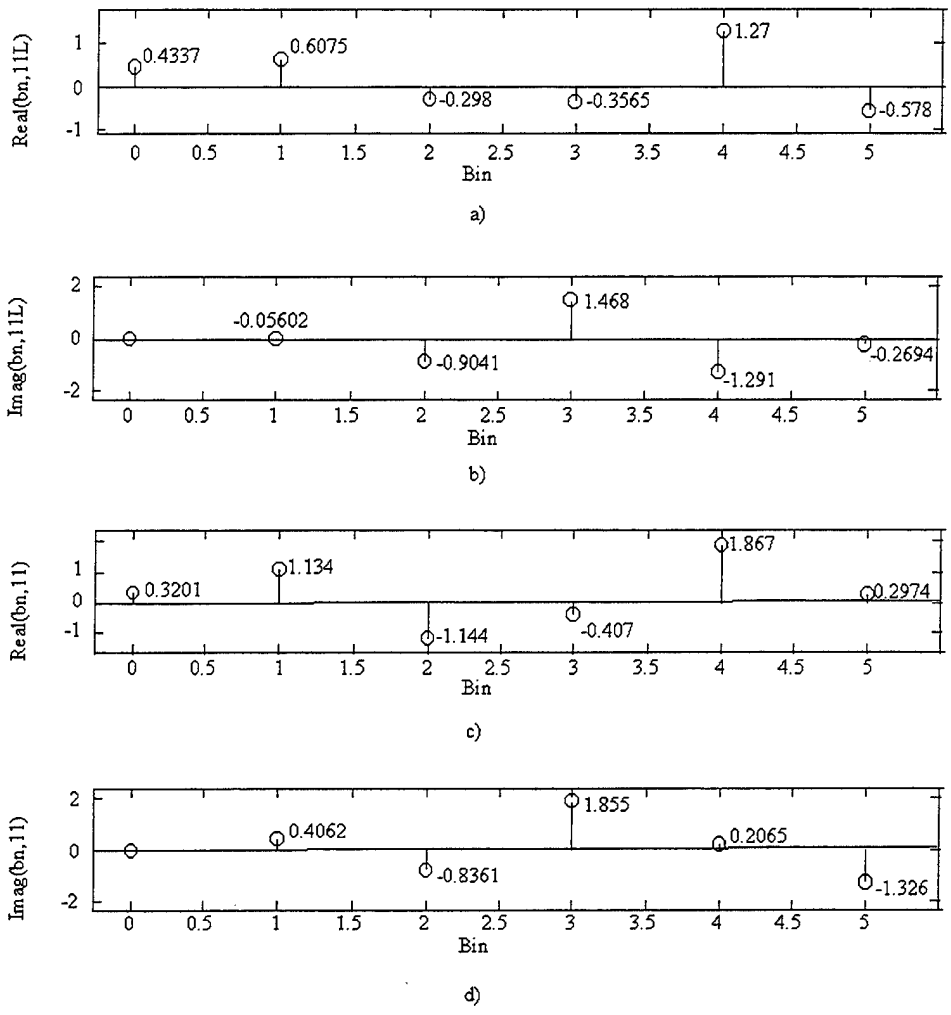

Figure 10.3: Spectra of a signal with frequency components from 0 to 10 Hz in 1/2 Hz increments: a) real component of sampled bandlimited signal, b) imaginary component of bandlimited signal, c) real component of sampled original signal, and d) imaginary component of original signal

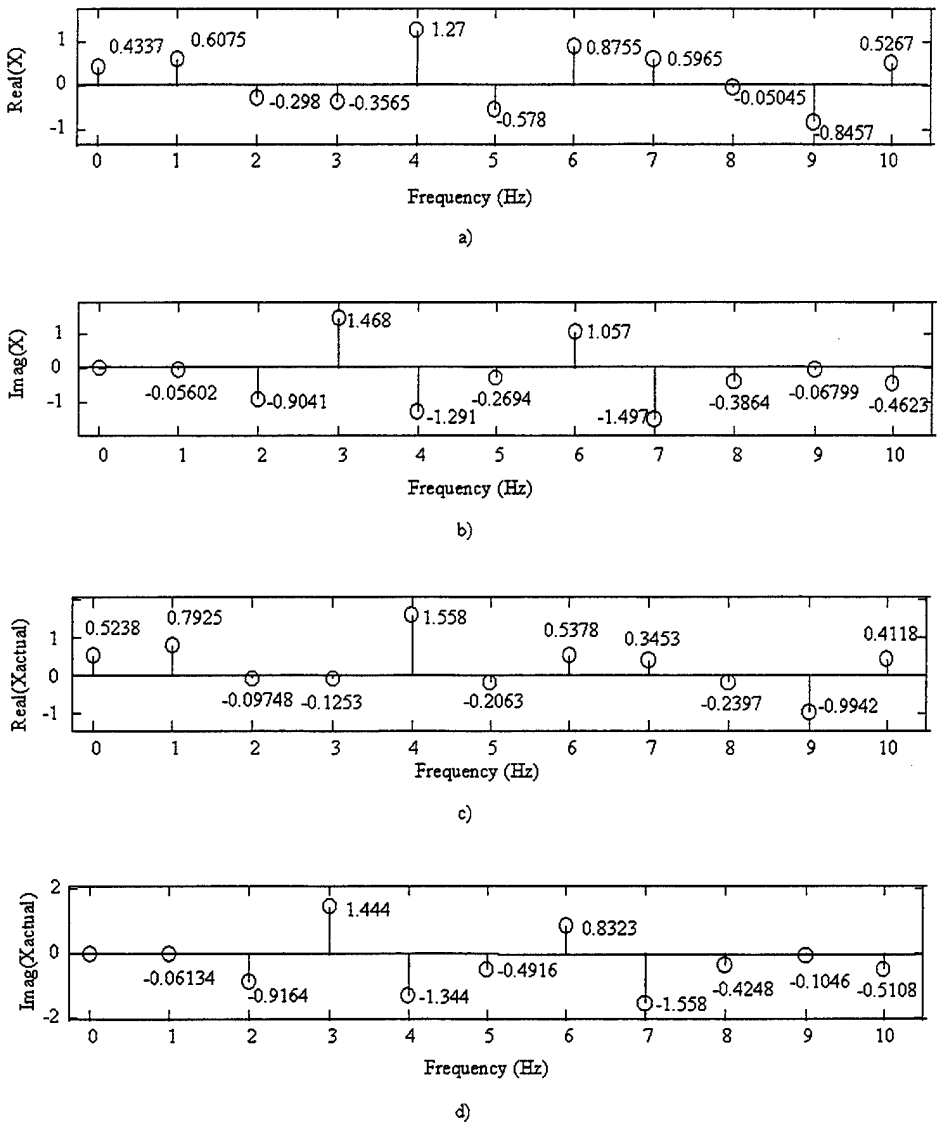

Figure 10.4: Spectra of a signal with frequency components from 0 to 10 Hz in 1/2 Hz increments: a) calculated real component, b) calculated imaginary component, c) actual real component, and d) actual imaginary component.

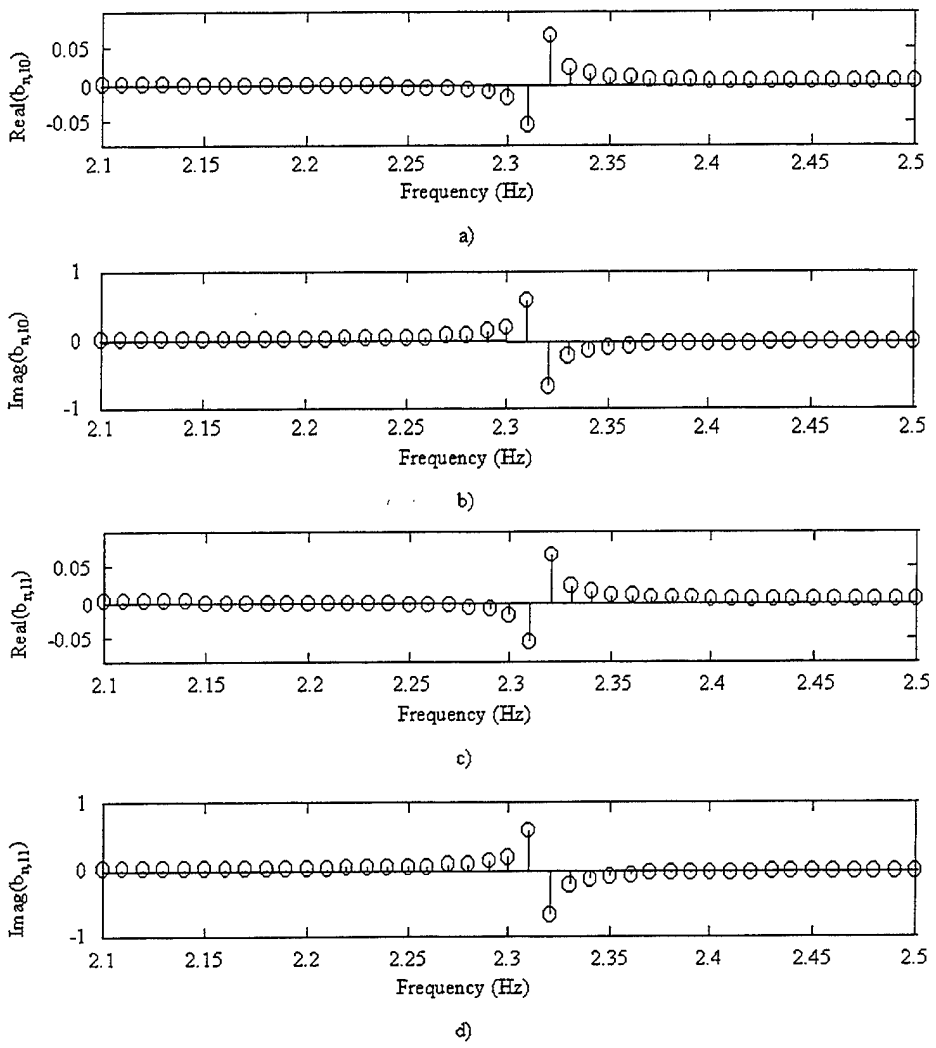

Figure 10.5: Normalized DFT with 0.01 Hz resolution of sinusoid at $f = 2.3153$ Hz: a) real component fo $f_{s1} = 10$ Hz, b) imaginary component for $f_{s1} = 10$ Hz, c) real component for $f_{s2} = 11$ Hz, and d) imaginary component for $f_{s2} = 11$ Hz.

XI. CONCLUDING REMARKS

The essential contribution of this thesis is detailing algorithms or solution methods that may hold the key to recovering an undersampled spectrum using one or more sampling frequencies. Using the Symmetrical Number System and the Discrete Fourier Transform it is a very simple process to resolve one or two undersampled frequencies within the dynamic range of the SNS. Additionally, when only resolving one or two frequencies, each pairwise relatively prime sampling frequency multiplicatively extends the dynamic range of the system. When resolving an entire spectrum of frequencies the solution becomes more complicated but it is still a straightforward process. The number of unique bins for each sampling frequency dictates the number of linearly independent equations that can be formed and hence dictates the dynamic range. Using at most two sampling frequencies demonstrated it has been shown that the spectral width that can be recovered using either method is approximately double the width predicted by Nyquist.

Future efforts will attempt to resolve two important questions. First, is it possible to apply the solution to a signal which has frequency components that don't conveniently lie directly at bin frequencies? The answer to this question may lie in increasing bin resolution and then using a mathematical method to determine fairly accurately the total energy that actually belongs to each integer frequency. The second question: What happens when more than two sampling frequencies are used? The matrix solution for two sampling frequencies is very simple and the solution matrix has nice properties. That may or may not be the case when three or more sampling frequencies are used.

In spite of problems that remain with the methods presented, the thesis is significant as it presents a direction for resolving an undersampled spectrum. Provided

that the leakage problem is solved, either or both of the methods may hold the key to greatly extending the ability to sample and resolve extremely high frequencies at relatively low sampling rates.

LIST OF REFERENCES

[1] J. Baier and H.W. Furst, "A Novel Method for Detection of Aliased Frequency Components in FFT-Based Spectrum Analyzers and Digital Oscilloscopes," *IEEE Proceedings*, Vol. 1, pp. 770-773, 1993.

[2] S. Barbarossa, "Parameter Estimation of Undersampled Signals by Wigner-Ville Analysis," *IEEE International Conference on Acoustics, Speech and Signal Processing*, Vol. 5, pp. 3253-3256, 1991.

[3] J.L. Brown Jr., "On the uniform sampling of a sinusoidal signal," *IEEE Trans. Aerospace and Electronic Systems*, Vol. 24, no. 1, pp. 103–106, Jan 1988.

[4] G. Hill, "The benefits of undersampling," *Electronic Design*, pp. 69–79, July 1994.

[5] R.E. Leino, P.E. Pace, and D. Styer, "Resolution of Multiple Frequency Undersampling Aliases," *IEEE Signal Processing Preprint.*

[6] R.D. Martin and D.J. Rasmussen, "A Testbed for Evaluating Undersampling Techniques," *IEEE Proceedings*, Vol. 1, pp. 157-164, 1992.

[7] I. Niven and H.S. Zukerman, *An Introduction to the Theory of Numbers*, 4th ed., John Wiley and Sons, New York, 1980.

[8] P.E. Pace, R.E. Leino, and D. Styer, "Use of the Symmetrical Number System in Resolving Single-Frequency Undersampling Aliases," *IEEE Signal Processing Preprint.*

[9] P.E. Pace, P.A. Ramamoorthy, and D. Styer, "A preprocessing architecture for resolution enhancement in high speed analog-to-digital converter," *IEEE Trans.*

Circuits and Systems II: Analog and Digital Signal Processing, Vol. 41, pp. 373–379, June 1994.

[10] C.M. Rader, "Recovery of Undersampled Periodic Waveforms," *IEEE Trans. Acoustics, Speech and Signal Proc.*, Vol. ASSP-25, no. 3, pp.242–249, Jun. 1977.

[11] J. Rozmaryn, "Undersampled wideband digital receiver," *Proc. Tri-Service DRFM-Digital Receiver Workshop*, 13–15 July, 1993.

[12] R.B. Sanderson, J.B.Y. Tsui, and N. Freese, "Reduction of aliasing ambiguities through phase relations," *IEEE Trans. Aerospace and Electronic Systems*, Vol. 28, no. 4, pp. 950–955, Oct. 1992.

[13] M.D. Zoltowski and Cherian P. Mathews, "Real-Time Frequency and 2-D Angle Estimation with Sub-Nyquist Spatio-Temporal Sampling," *IEEE Transactions on Signal Processing*, Vol. 42, no. 10, Oct. 1994.

INITIAL DISTRIBUTION LIST

	No. Copies
1. Defense Technical Information Center 8725 John J. Kingman Road, Ste 0944 Fort Belvoir, VA 22060-6218	2
2. Dudley Knox Library Naval Postgraduate School 411 Dyer Rd. Monterey, California 93943-5101	2
3. Chairman, Code EC Department of Electrical and Computer Engineering Naval Postgraduate School Monterey, California 93943-5121	1
4. Professor Phillip E. Pace, Code EC/Pc Department of Electrical and Computer Engineering Naval Postgraduate School Monterey, California 93943-5121	3
5. Professor David Styer Department of Mathematical Sciences The University of Cincinnati, ML 25 Cincinnati, OH 45221	1
6. Captain Richard E. Leino USMC 9801 Portside Dr. Burke, VA 22015	4
7. Space and Naval Warfare Systems Command Department of the Navy PMW-178 Attn: Captain Ristorcelli Washington, DC 20363-5100	1
8. Space and Naval Warfare Systems Command Department of the Navy PMW-163 Attn: Captain Connell Washington, DC 20363-5100	1

No. Copies

9. Rome Laboratory/IRAP — 1
   Attn: Bill Ziesenitz
   32 Hangar Road
   Griffiss AFB, NY 13441-4114

10. Director, Training and Education — 1
    MCCDC, Code C46
    1019 Elliot Road
    Quantico, Virginia 22134-5027

11. Director, Marine Corps Research Center — 2
    MCCDC, Code C40RC
    2040 Broadway Street
    Quantico, Virginia 22134-5107

12. Director, Studies and Analysis Division — 1
    MCCDC, Code C45
    300 Russell Road
    Quantico, Virginia 22134-5130